# Theory and Application of Software Defined Electronics:

## Design Concepts for the Next Generation of Telecommunications and Measurement Systems

Géza Kolumbán, Tamás István Krébesz, and Francis C.M. Lau

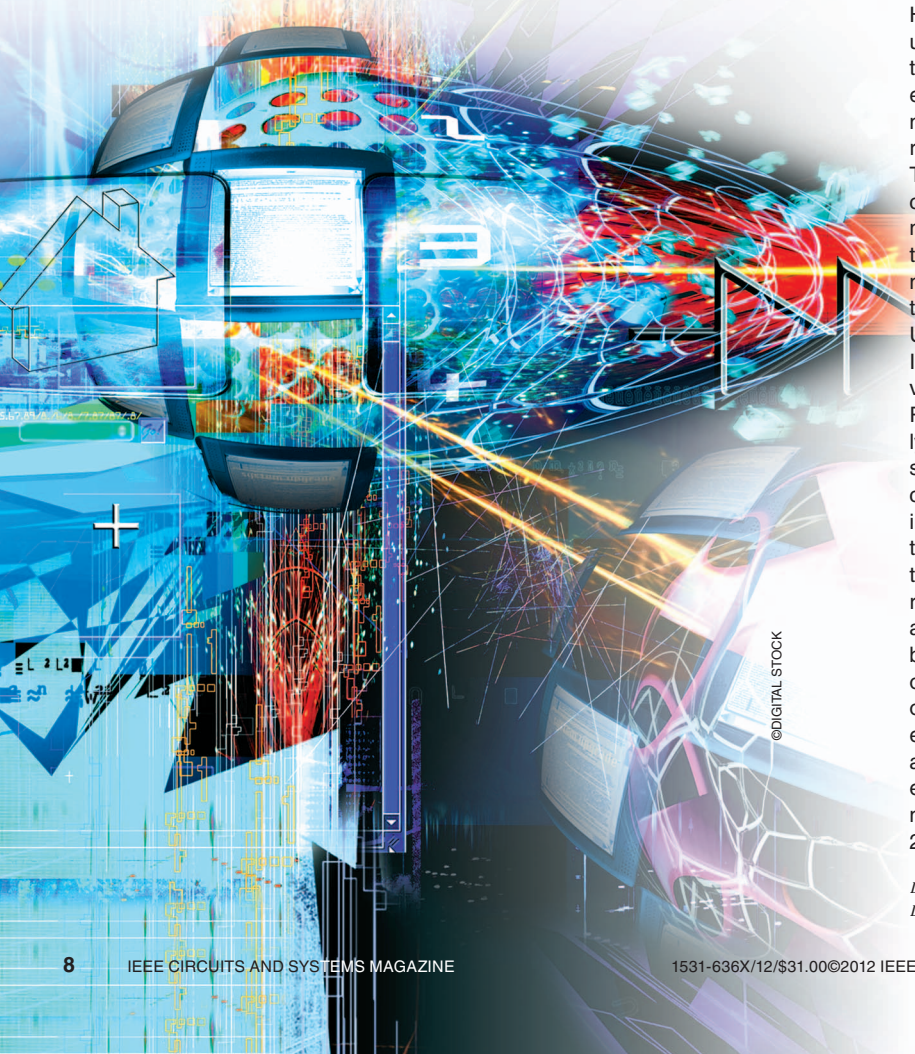

©DIGITAL STOCK


### Abstract

The analog signal processing is substituted everywhere by its digital counterpart because of its higher accuracy and flexibility, its much lower cost and because in digital signal processing there is no need for regular calibration as it is required in the analog systems. The most important feature of digital approach is that the HW and SW components can be fully separated and the same HW, referred to as a universal HW device, can be used to implement very different applications. Although digital signal processing has been around everywhere in the low frequency applications for many years, until this time it could not satisfy the requirements of RF and microwave engineering. The main challenges in RF and microwave radio communications and measurements are: (i) implementation of ultra wide dynamic range (limited by the quantization noise and linearity) and (ii) minimize sampling rate required. In our time the situation is changing rapidly. Software Defined Radio, Universal Software Radio Peripheral and Virtual Instrumentation all mean that a universal HW device is used to extract the complex envelope of an RF bandpass signal to be demodulated or analyzed, and the implementation of radio receiver or signal analyzer is implemented entirely in SW. The complex envelope, processed in SW, carries all information available in the RF signal and assures the minimum sampling rate which is determined by the bandwidth of RF signal. The complex envelope represents fully the RF bandpass signal without any distortion and every RF bandpass signal can be reconstructed from its complex envelope without any distortion. This tutorial surveys the theory of complex envelopes, shows how the baseband equivalent models of RF systems can be derived and demonstrates how different radio transceivers and test equipment can be implemented by means of the same universal RF HW device in the 2.4-GHz ISM frequency band.


*Digital Object Identifier 10.1109/MCAS.2012.2193435*
*Date of publication: 22 May 2012*

 1531-636X/12/$31.00©2012 IEEE 

## I. Introduction

Signal processing algorithms are used to generate and analyze signals in order to transfer information or to measure some parameters via information extraction. The former and latter are performed in telecommunications and measurement engineering, respectively. Until recently, the signal processing algorithms have been implemented mostly by analog circuits in the microwave and Radio Frequency (RF) regions. To simplify the terminology, the microwave and RF regions will not be distinguished in the remaining part of tutorial.

The general trend in computer science and electrical engineering is that the HardWare (HW) and SoftWare (SW) components are becoming completely separated and only one, or a very few universal HW devices are used to implement many different applications just changing the SW in the application layer. The idea of HW-SW separation is well known but until now cheap and universal HW devices have not been available in the RF regions because high sampling rate and resolution are required in telecommunications and measurement engineering applications.

Bandpass signals are used in RF telecommunications and measurement engineering where the center frequency of the signal to be processed is much greater than its bandwidth. According to the Raabe condition, the sampling rate has to be higher than twice the bandwidth of RF bandpass signal. Note, the required sampling rate is determined not by the center frequency but by the bandwidth of RF bandpass signal.

The canonical representation of bandpass signals and systems introduced by the concept of complex envelopes makes the BaseBand (BB) representation possible showing that every RF bandpass signal (either deterministic or random) and system can be fully represented in the lowpass region where the bandwidth of BB equivalent is equal to the half of that of the original signal or system. Note, the BB equivalents are not approximations but exact representations of the original signals and systems, consequently, distortion does not occur.

The Raabe condition establishes the theoretical possibility of substituting every RF bandpass signal processing performed up to now by analog circuitry in RF domain with a digital one in baseband, furthermore, the concept of complex envelopes provides the theory which is necessary to derive design equations and methods for the circuit and system design in baseband. Although the Raabe condition and the concept of complex envelopes, also referred to as analytic signals, have been available for many decades, until now universal HW devices which can extract the complex envelope from the RF bandpass signal to be processed and which can reconstruct the RF bandpass signal from its complex envelope have not yet been available on the market. This situation has changed recently with the advent of cheap integrated circuits which can perform the transformation between the RF domain and baseband. Even more, devices referred to as Universal Software Radio Peripherals (USRPs) are now available that implement a physical layer and that can be accessed via two service access points: the (i) USRP management service and (ii) USRP data service access points. The USRP devices are suitable for embedded operation and can be driven directly from a suitable software run in the application layer.

The USRP devices are universal in that sense that together with a host computer they can perform any kinds of RF bandpass signal processing, consequently, they are suitable for the implementation of any kinds of telecommunications systems or measurement equipment. The crucial issue is the derivation of equivalent baseband model, more precisely, the derivation of equivalent BB algorithm that has to be implemented in the application layer. Unfortunately, a publication on the systematic derivation of equivalent BB algorithm cannot be found in the literature.

This tutorial is going to fulfill this gap.

Chapter II surveys the complex envelope representation of signals, random processes and Linear Time Invariant (LTI) systems. The discussion is rigid from a mathematical point of view, but focuses on the applications and implementations, consequently, many details are not discussed and mathematical proofs are not given. However, every theorem necessary to derive the BB equivalents are provided.

Chapter III introduces the universal HW device that can process or generate the RF bandpass signals and that provides the interface to the upper application

*Géza Kolumbán is with the Faculty of Information Technology, Pázmány Péter Catholic University, Budapest, Hungary. E-mail: kolumban@itk.ppke.hu. Tamás István Krébesz is with the Department of Measurement and Information Systems, Budapest University of Technology and Economics, Budapest, Hungary. E-mail: krebesz@mit.bme.hu. Francis C.M. Lau is with the Department of Electronic and Information Engineering, The Hong Kong Polytechnic University, Hong Kong SAR, China. E-mail: encmlau@polyu.edu.hk.*

**Like computer science, the advent of Universal Software Radio Peripheral (USRP) makes the complete separation of HW and SW components possible in RF telecommunications and measurement engineering.**

layer. The drivers establishing the access points for the application layer are also discussed.

Chapter IV surveys the features of SW-based BB signal processing.

Every radio link includes a (i) transmitter, a (ii) radio channel and a (iii) receiver. Chapter V shows the derivation of BB equivalents of analog and digital transmitters, the implementation of different radio channels such as ideal noise-free channel, Additive White Gaussian Noise (AWGN) channel and two-ray noisy multipath channel, and the derivation of BB equivalent of a generic QPSK demodulator. Finally, to show all features of complex envelope concept, a complete half-sine O-QPSK radio link communicating over the three radio channels listed above is implemented. A step-by-step approach is shown to derive the BB equivalents and the discussion goes from the simplest case to the most complex case. The implementations to be discussed cover all signal processing tasks to be done in radio communications, consequently, using the tools discussed here the reader will be able to derive the BB algorithm for his or her own problem.

The modulated signal radiated by the transmitter can also be considered as a test signal which can be used to measure the characteristics of a radio channel or an entire radio link. A great feature of Software Defined Electronics (SDE) is that signal processing is implemented in SW, consequently, one algorithm can demodulate the received signal, while other algorithms, run parallel, can determine the spectrum of received signal or plot the constellation diagram without interrupting the data traffic. This feature being essential in cognitive radio is also demonstrated in Chapter V.

Constituting ideas of SDE concept has been used for many years in software defined radio, virtual instrumentation, open system interconnection basic reference model, embedded systems and in the concept of complex envelopes. However, until this time these areas have been treated more or less independently of one another because a universal HW device has not been available up to now. With the advent of universal HW device, the SDE concept integrates these areas into one unified approach and is causing a change in design paradigm of microwave and RF telecommunications systems and measurement equipment.

SDE approach can be used in new product development because it reduces the time to market and also offers a simple and fast solution for testing new protocols and communications approaches. In research the SDE approach offers a unified test bed for verification of new theoretical ideas and practical solutions. The use of universal HW device makes the development of microwave circuit unnecessary, that requires a very special knowledge and expensive measurement equipment.

Last but not least SDE establishes a brand new research direction for the IEEE Circuits and Systems Society. New equivalent baseband algorithms optimized for the FPGA-based digital signal processing have to be developed. The high-speed FPGA devices are resource-limited computing devices where fixed-point number representation and fixed-point arithmetics are used. This framework has some serious limitations but also offers new opportunities in the algorithm design. As the circuits and systems were developed in the past by the IEEE CAS Society, now the derivation of new equivalent BB algorithms is challenging the CAS Society.

## II. Basic Issues: Complex Envelope Representations of Signals, Noise, and LTI Systems

During the analysis of a telecommunications system we have to consider three basic components:

- signals that carry the information
- LTI blocks that are used to process the signals carrying the information
- random processes that are used to model the channel noise or interference.

The constituting blocks of a test equipment are the same, the only difference is that in measurements the noise is generated by the test bed and the source of interferences can be any kind of signal generators.

The constituting blocks of telecommunications systems and test beds are assumed to be linear at the system level analysis, the nonlinearities are considered only as secondary unwanted effects. This paper is going to show how the BB equivalent of an RF bandpass system developed for either telecommunications or measurement engineering application can be derived, the modeling of nonlinearities goes beyond the scope.

Chapter II surveys the theory of complex envelopes. Only those definitions and theorems will be discussed that are needed to derive the BB equivalent of an RF bandpass systems. The proofs of theorems will not be provided but every equations and statements will be

exact from a mathematical point of view. For details the interested readers should refer to the literature [1]–[3].

Originally, the terminology of baseband and lowpass has been introduced for the linear and nonlinear modulation schemes, respectively. This distinction has been fading away and baseband will be considered as a synonym to lowpass in this paper.

### *A. Definition of Complex Envelope*

Consider a bandpass, typically but not necessarily RF signal $x(t)$ with an RF bandwidth of $2B$ centered about a center frequency $f_c$ with its Fourier transform $X(f)$. The spectrum of RF bandpass signal is depicted in Fig. 1. The only constrain that has to be satisfied during the BB representation is that the half of RF bandwidth should not be greater than the center frequency

$$B \leq f_c.$$

This tutorial focuses on the RF bandpass signal processing, to clearly distinguish the RF bandpass signals from their BB equivalents the terminology of "RF bandpass" will be used everywhere.

To get the complex envelope of $x(t)$[1], the RF bandpass signal is decomposed into a slowly-varying *complex envelope*

$$\tilde{x}(t) = x_I(t) + jx_Q(t) \tag{1}$$

and an exponential signal $\exp(j\omega_c t)$ as defined by

$$x(t) = \Re[\tilde{x}(t)\exp(j\omega_c t)]. \tag{2}$$

The real and imaginary components of complex envelope are denoted by $x_I(t)$ and $x_Q(t)$, respectively. Note, both of them are real-valued signals.

Our aim is to process the complex envelope, i.e., the equivalent BB signal by digital signal processing. To minimize the required sampling rate in BB, $f_c$ has to be set to the center frequency of the RF frequency band to be considered. In case of a modulated RF signal $f_c$ is equal to the carrier frequency.

In the time domain the decomposition of RF bandpass signal defined by (2), provides a slowly varying complex envelope $\tilde{x}(t)$ which, except the center frequency, carries all the information that is available in the original RF bandpass signal. The digital processing of slowly varying complex envelope requires only a low

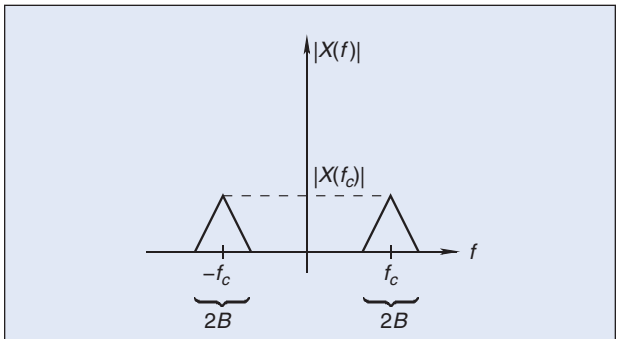


**Figure 1.** Spectrum of RF bandpass signal to be represented in baseband.

sampling rate. The transformation into the baseband can be also observed in the frequency domain, Fig. 2 depicts the spectrum of complex envelope. The spectrum has a lowpass characteristic and its bandwidth $B$ is the half of that of the RF bandpass signal. The frequency region about zero frequency is covered by the spectrum of complex envelope and referred to as baseband. Note, in case of equivalent baseband signal processing the required sampling rate is determined by $B$, i.e., by the half of RF bandwidth.

The complex envelope offers the following features:

- Except the center frequency $f_c$, the complex envelope $\tilde{x}(t)$, given in BB, carries all the information available in the RF bandpass signal.
- It is a *representation*, i.e., the RF bandpass signal can be fully reconstructed, without any distortion, from its complex envelope.
- The complex envelope assures the attainable minimum sampling rate in digital signal processing.
- The price that has to be paid for the BB representation and minimum sampling rate is that the complex envelope is not a real- but a *complex-valued* function.

Derivation of complex envelope is a two-step process where first the pre-envelope has to be defined by means of the Hilbert transform and then the one-sided spectrum of complex envelope is shifted to BB to get the

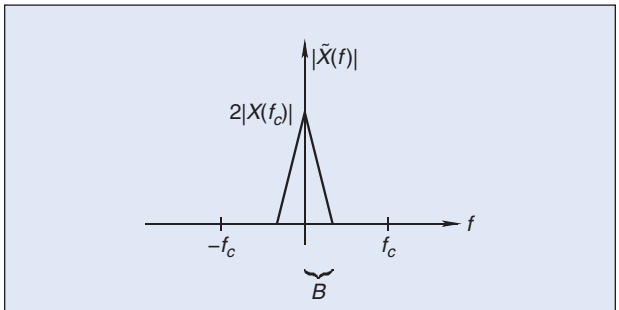


**Figure 2.** Spectrum of complex envelope in the baseband.

[1] Two similar but different definitions are given in the literature for the complex envelope. In the first version given in [1] and [2] the extracted carrier is a pure exponential, $\exp(j\omega_c t)$, while in the second version the extracted carrier includes $\sqrt{2}$, i.e. it is $\sqrt{2}\exp(j\omega_c t)$ [3]. The latter approach is a generalization of the phasor concept.

Since LabVIEW uses the first version of definition, (2) will be applied here.

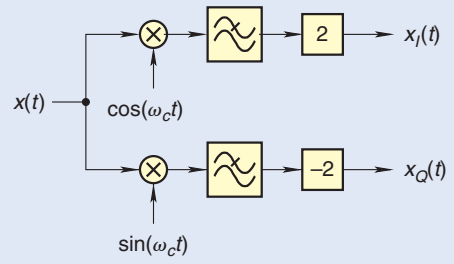


**Figure 3.** Generation of complex envelope $\tilde{x}(t) = x_I(t) + jx_Q(t)$ from the RF bandpass signal $x(t)$.

complex envelope. These steps involve a lot of mathematics [1]. However, if one is interested only in the application of equivalent BB signal processing then it is enough to use two block diagrams; the former has to be used to extract the complex envelope from an RF bandpass signal to be processed, while the latter has to be used to reconstruct an RF bandpass signal from its complex envelope. These block diagrams will be discussed in the next two sections.

### *B. Generation of Complex Envelope*

As its name says the complex envelope is a complex-valued signal. A complex-valued signal can be manipulated directly in digital signal processing performed on a computer or FPGA, but the built circuits can process only real-valued signals.

In built circuits, two parallel signal processing arms, referred to as *in-phase* and a *quadrature* arms are used, where the former and latter manipulate the real and imaginary components, respectively, of complex envelope. To distinguish the real-valued RF bandpass and BB complex-valued signals clearly we will plot both the in-phase and quadrature arms in our block diagrams.

The complex envelope can be extracted from an RF bandpass signal to be processed by a (i) quadrature mixer, (ii) two lowpass filters and (iii) two amplifiers as shown in Fig. 3.

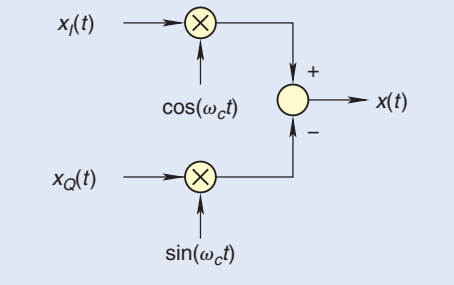


**Figure 4.** Reconstruction of RF bandpass signal $x(t)$ from its complex envelope $\tilde{x}(t)$.

In the block diagram, in general, the upper and lower arms denote the in-phase and quadrature arms, respectively. But this notation is not always followed, note, the type of arm is determined by the phase of local signal, the signals of in-phase and quadrature arms appears at the output of the mixers driven by the *cosine* and *sine* local signals, respectively.

### *C. Reconstruction of RF Bandpass Signal*

Substituting (1) into (2), the RF bandpass signal is obtained in *canonical* form

$$x(t) = x_I(t)\cos(\omega_c t) - x_Q(t)\sin(\omega_c t). \tag{3}$$

This equation defines the algorithm for the reconstruction of the RF bandpass signal. The block diagram implementing (3) is depicted in Fig. 4 where a quadrature mixer and an adder are used to reconstruct the RF bandpass signal from its complex envelope.

### *D. Definition of Envelope and Phase of an RF Bandpass Signal*

The complex envelope representation gives an exact mathematical definition for the *envelope* and *angle* of an RF bandpass signal. Since in telecommunications the information to be transmitted is carried by the amplitude or angle, or both, of a sinusoidal carrier, this definition is extremely important in signal processing and system level analysis of telecommunications systems.

The complex envelope can be expressed either in Cartesian or polar form

$$\tilde{x}(t) = x_I(t) + jx_Q(t) = a(t)\exp[j\theta(t)]. \tag{4}$$

Substituting (4) into (2), the envelope and angle of an RF bandpass signal is defined as

$$\begin{aligned} x(t) &= \Re[\tilde{x}(t)\exp(j\omega_c t)] = \Re[a(t)\exp(j[\omega_C t + \theta(t)])] \\ &= a(t)\cos[\omega_C t + \theta(t)]. \end{aligned} \tag{5}$$

By definition, the information to be transmitted is mapped into the envelope of RF carrier in case of Amplitude Modulation (AM)

$$a(t) = |\tilde{x}(t)| = \sqrt{x_I^2(t) + x_Q^2(t)} \tag{6}$$

into the phase of RF carrier in case of Phase Modulation (PM)

$$\theta(t) = \arctan\left[\frac{x_Q(t)}{x_I(t)}\right] = \Im(\ln[\tilde{x}(t)]) \tag{7}$$

and into the difference measured between the instantaneous frequency of RF modulated waveform and its carrier frequency $f_c$ in case of Frequency Modulation (FM)

$$\frac{d\theta(t)}{dt} = \frac{d}{dt}\left(\arctan\left[\frac{x_Q(t)}{x_I(t)}\right]\right). \tag{8}$$

Many times the desired signal is corrupted by an interference or any kind of unwanted RF bandpass signal. During the system level analysis we have to evaluate the effect of unwanted signal on the demodulator output. The complex envelope representation gives not only a mathematical definition for the envelope and angle of an RF bandpass signal but it also shows how this arbitrary unwanted RF bandpass signal can be taken into account during the analysis.

Every receiver is designed in such a way that it is sensitive only to a certain type of modulation. For example, in an FSK receiver a hard limiter that removes the AM completely from the received signal precedes the FSK demodulator which is sensitive only to FM carried by the received signal. Unfortunately, the channel filter passes both the desired and the unwanted signals because their spectra overlap one another. To determine the receiver sensitivity to the unwanted signal, a mathematical model has to be found.

Equation (4) gives a clue to the solution. Let $x(t)$ denote the unwanted signal passed by the channel filter. The channel filter output is an RF bandpass signal. Then according to the RHS of (4), $x(t)$ is decomposed into an envelope and angle denoted by $a(t)$ and $\theta(t)$, respectively. The variation in envelope, i.e., the AM is removed by the hard limiter. From the angle $\theta(t)$ the FM generated by the unwanted signal can be determined as shown by (8). This unwanted FM will generate the interference in the demodulated message.

Note this approach can be applied to any kind of unwanted signals, either a modulated waveform or an RF bandpass signal.

### *E. Complex Impulse Response of LTI Systems*

The output signal of an LTI system is expressed as the convolution of the input signal $x(t)$ and its impulse response $h(t)$ as shown in Fig. 5(a). To perform the signal processing completely in baseband, a direct relationship between the complex envelopes of input and output RF bandpass signals of LTI two-port has to be established in a similar form as shown in Fig. 5(b).

Let $\tilde{x}(t)$ and $\tilde{y}(t)$ denote the complex envelopes of RF bandpass signals measured at the input and output, respectively, of RF bandpass LTI two-port. Then the *complex impulse response* of RF bandpass two-port is derived as that of a bandpass signal [1] and takes the form

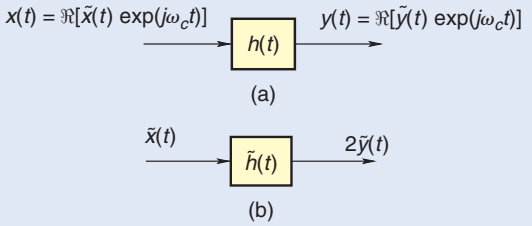


**Figure 5.** LTI systems are completely characterized by their (a) impulse response and their (b) complex impulse response in the RF bandpass and BB domains, respectively.

$$h(t) = \Re[\tilde{h}(t)\exp(j\omega_c t)] = \Re\{[h_I(t) + jh_Q(t)]\exp(j\omega_c t)\}. \tag{9}$$

The complex envelope of LTI output is also obtained by convolution

$$\tilde{y}(t) = \frac{1}{2}\int_{-\infty}^{\infty}\tilde{h}(\tau)\tilde{x}(t-\tau)\,d\tau = \frac{1}{2}\tilde{h}(t) \star \tilde{x}(t), \tag{10}$$

where $\star$ denotes the convolution. Formally, (10) is identical to the convolution integral used in the analysis of LTI systems, however, note two crucial differences:

- convolution integral returns twofold of complex envelope measured at the LTI output and
- in Fig. 5(b) both $\tilde{x}(t)$ and $\tilde{h}(t)$ are complex valued functions.

Consequently, the evaluation of (10) requires the calculation of four real-valued convolution integrals as shown in Fig. 6.

A useful practical tip: In many applications bandpass filters are used only to select a specified frequency band and suppress the signals outside the desired frequency band. A bandpass filter with zero-phase can be used to perform this task. Zero-phase filters [4] have a very important advantage, namely, for them $h_Q(t) = 0$.

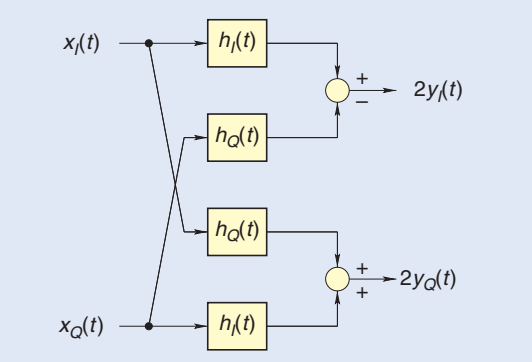


**Figure 6.** The convolution of two complex-valued functions require the evaluation of four real-valued convolution integrals.

Consequently, the four real-valued correlations defined by (9) are simplified into two real-valued correlations as shown in Fig. 7. Note, for the zero-phase filters $h_Q(t) = 0$ which means physically that the cross couplings between the in-phase and quadrature arms are becoming zero.

### *F. Representation of Gaussian RF Bandpass Random Process*

Gaussian random process plays a central role in the analysis and design of telecommunications and measurement systems because

- It has a normal distribution that can be fully characterized by the mean and variance;
- If a Gaussian process is processed by an LTI system then the output is also a Gaussian random process;
- In LTI systems, Gaussian process makes the derivation of results in analytical form possible.

RF bandpass Gaussian random processes are frequently used to model the effect of channel noise and interferences. A distinction will not be made here between noise and interference, the sample function of both random processes is denoted by $n(t)$.

The complex envelope approach can be applied only to bandpass signals and systems. If we want to extend the theory of complex envelopes to the Gaussian random process then we have to form a band limited process.

The most frequently used channel model in telecommunications engineering is the AWGN channel model. Unfortunately, the white noise is not a bandpass noise.

Let $W(t)$ and $N(t)$ denote two random processes characterized by their sample functions $w(t)$ and $n(t)$. Let $W(t)$ be a Gaussian random process of zero mean and uniform Power Spectral Density (psd). Note, $w(t)$ is the sample function of a white Gaussian noise.

Let $w(t)$ be filtered by an ideal bandpass filter having an RF bandwidth of $2B_{\text{noise}}$ and let the output of the bandpass filter be denoted by $n(t)$. Since $2B_{\text{noise}} \geq 2B$, where $2B$ denotes the bandwidth of RF bandpass signal to be processed, this bandpass filtering that makes the BB modeling of Gaussian process possible does not have any effect on the RF bandpass signal to be processed.

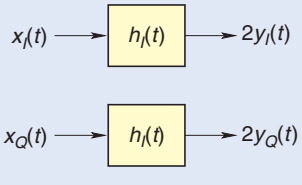


**Figure 7.** For zero phase filters $h_Q(t) = 0$ and only two real-valued convolution integrals have to be evaluated.

The bandpass RF random process $N(t)$ has the following characteristics:

- It is a Gaussian random process with zero mean;
- It is an RF bandpass process and its psd has a bandwidth of $2B_{\text{noise}} \geq 2B$ centered about the center frequencies $\pm f_c$.

Assume that the psd of $N(t)$ is locally symmetric about the center frequencies $\pm f_c$ and let $R_n(\tau)$ denote the autocorrelation function of bandpass random process $N(t)$.

Like every band-pass signal and system, $n(t)$ can also be represented by its complex envelope [1]

$$\begin{aligned} n(t) &= \Re[\tilde{n}(t)\exp(j\omega_C t)] \\ &= \Re\{[n_I(t) + n_Q(t)]\exp(j\omega_C t)\}. \end{aligned} \tag{11}$$

The sample function $n(t)$ can be expressed either in canonical form or as a modulated signal

$$\begin{aligned} n(t) &= n_I(t)\cos(\omega_C t) - n_Q(t)\sin(\omega_C t) \\ &= a_n(t)\cos(\omega_C t + \theta_n), \end{aligned} \tag{12}$$

where the following equations give the definition for the envelope

$$a_n(t) = \sqrt{n_I^2(t) + n_Q^2(t)} \tag{13}$$

and the phase

$$\theta_n(t) = \arctan\left[\frac{n_Q(t)}{n_I(t)}\right] \tag{14}$$

of the random processes $N(t)$.

The RHS of (12) has a crucial importance in the analysis of telecommunications systems because it shows how a random process can be decomposed into an amplitude and phase modulation. This decomposition is used when, for example, the effect of local noise has to be evaluated. The modulations $a_n(t)$ and $\theta_n(t)$ are referred to as amplitude and phase noise.

As explained in Sec. II-D our receivers or test equipment are sensitive, in general, only to a certain type of modulation. The other types of modulations are suppressed by limiters or envelope detectors just to mention two examples.

Assume that the system under study has got an envelope detector. Then the local noise is decomposed into amplitude and phase noise components and only the amplitude noise is considered. The phase noise, because it has no influence on the output of the envelope detector is disregarded.

Let $R_n(\tau)$ and $R_{n_I}(\tau)/R_{n_Q}(\tau)$ denote the autocorrelation functions of $N(t)$ and $N_I(t)/N_Q(t)$ random processes, respectively. Recall, the outcomes of these random processes are denoted by $n(t)$ and $n_I(t)/n_Q(t)$, respectively.

**USRP is a computer-hosted universal hardware platform for the implementation of software defined radio or virtual instrumentation. It performs the transformation between the RF domain and baseband.**

The relationship among these autocorrelation functions is obtained as [1]

$$R_n(\tau) = R_{n_I}(\tau)\cos(\omega_C\tau) = R_{n_Q}(\tau)\cos(\omega_C\tau), \quad (15)$$

where

$$R_{n_I}(\tau) = R_{n_Q}(\tau).$$

Observe, (11) claims that the lowpass equivalent of Gaussian RF bandpass random processes can be generated directly in baseband. Two Pseudo Random Number Generators (PRNGs) have to be used in BB, one to generate the in-phase component $n_I(t)$ and a second one to provide the quadrature component $n_Q(t)$. The properties of the generated two PRN sequences are summarized below:

1) If $N(t)$ is a Gaussian process and is stationary in wide-sense, then random processes $N_I(t)$ and $N_Q(t)$ are jointly Gaussian and jointly stationary in wide-sense.
2) Since sample function $n(t)$ has zero mean, both $n_I(t)$ and $n_Q(t)$ have zero mean values.
3) The in-phase and quadrature components have the same variance as the RF bandpass noise. Recall, variance gives the noise power.
4) The correlation functions of $n_I(t)$ and $n_Q(t)$ obey the following equations

$$\overline{n_I(t)n_I(t+\tau)} = R_{n_I}(\tau) \equiv R_{n_Q}(\tau) = \overline{n_Q(t)n_Q(t+\tau)} \quad (16)$$

and

$$\overline{n_I(t)n_Q(t+\tau)} = -\overline{n_Q(t)n_I(t+\tau)} = 0, \quad (17)$$

where overbar symbolizes the time-averaging operation.

5) Since $R_{n_I}(\tau) = R_{n_Q}(\tau)$, both the in-phase and quadrature noise components have the same psd that is related to the psd $S_N(f)$ of RF bandpass random process $N(t)$ as

$$S_{N_I}(f) = S_{N_Q}(f) = \begin{cases} S_N(f-f_C) + S_N(f+f_C), & -B \le f \le B \\ 0, & \text{elsewhere} \end{cases}, \quad (18)$$

where $S_N(f)$ is zero outside the frequency band $f_C - B \le |f| \le f_C + B$ and $f_C > B$.

Properties summarized above are extremely important when the BB equivalent of an RF bandpass random process is generated because they give detailed instruction how the parameters of BB PRNGs have to be determined

- Two PRNGs have to be used to generate the random processes denoted by $n_I(t)$ and $n_Q(t)$.
- According to (16), the autocorrelation functions of the two random sequences have to be equal to each other. Please note, this implies that the psd and variance (or power) of the two random sequences have to be identical.
- However, (17) shows that $n_I(t)$ and $n_Q(t)$ must be independent, i.e., orthogonal. The generation of two orthogonal sequences by means of one PRNG algorithm requires the use of independent seeds, otherwise the generated sequences will be correlated. Please note, any correlation seriously corrupts the result of simulation.

## III. Hardware Platform of Implementation: The USRP Approach

Universal Software Radio Peripheral [5] is a computer-hosted hardware platform for the implementation of software defined radio or low-accuracy virtual instrumentation. Each USRP device includes a receive (Rx) and transmit (Tx) block, these blocks correspond to the block diagrams introduced to generate the complex envelope and reconstruct the RF bandpass signal from its complex envelope, depicted in Figs. 3 and 4, respectively.

The USRP approach relies on equivalent BB signal processing of RF bandpass signals. It performs all the waveform-specific signal processing steps, such as modulation and demodulation, in BB on a host-computer while all the general purpose operations requiring high-speed data processing, such as interpolation and decimation, are carried out on an FPGA available on the main board of USRP device.

### *A. Hardware Architecture of USRP*

The USRP device, whose block diagram is shown in Fig. 8, includes two essential components, (i) the *main board*- carrying the FPGA, the digital-to-analog (DAC) and analog-to-digital (ADC) converters, and a standard interface between the host-computer and the USRP unit- and (ii) the *RF transceiver daughter-board* that generates the complex envelope from the received RF driving the ADCs in receive mode and reconstructs the RF signal to be transmitted from the complex envelope provided by DACs.

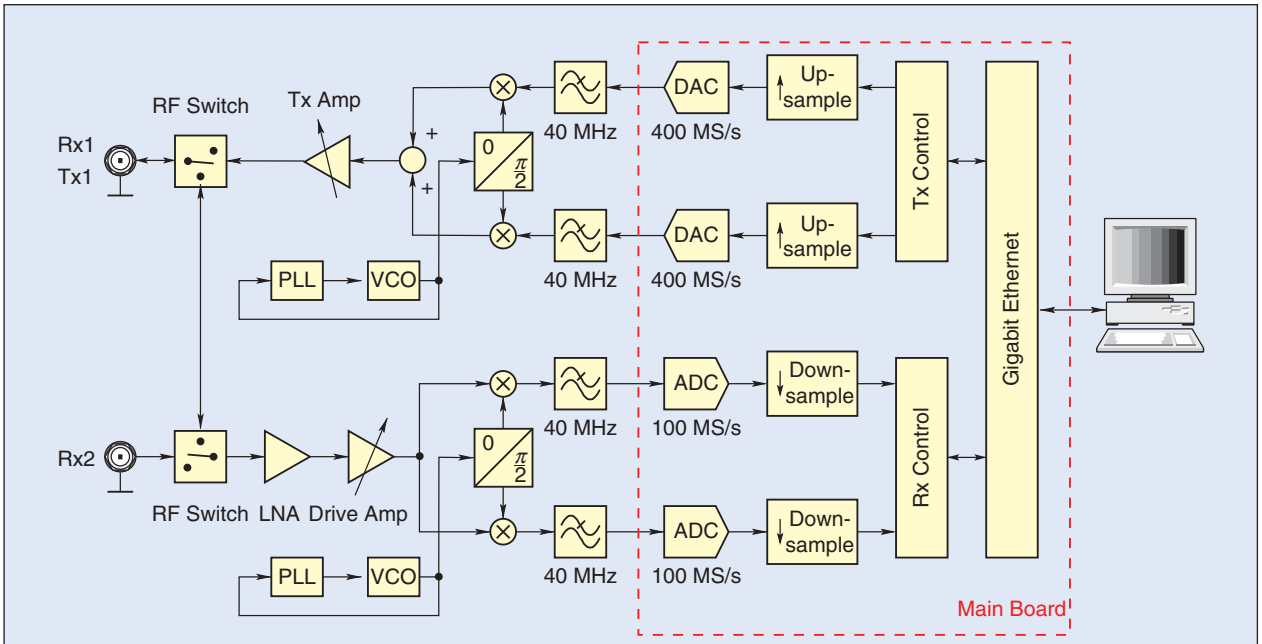


**Figure 8.** Typical block diagram of a USRP device.

The USRP device is connected to the host computer via a Gigabit Ethernet interface that is managed by an open source Medium Access Control (MAC) layer implemented on the FPGA and by a National Semiconductor Ethernet Physical (PHY) layer chip. The FPGA, a Xilinx Spartan 3, is responsible for the MAC layer management of the Gigabit Ethernet, for controlling and packetizing *in-phase (I)* and *quadrature (Q)* samples and for performing downsampling and upsampling.

**1. Receive Block of USRP Device**

The USRP device has two SMA connectors for the RF bandpass signals and it can operate either in simplex or duplex mode. Two RF switches are used to select the required configuration, the receive antenna may be connected to the inputs Rx1 and Rx2, while the transmitter output always appears at the Tx connector.

The weak received signal is fed into a low-noise amplifier (LNA). Its role is twofold: (i) to minimize the noise figure of the receiver and (ii) to raise the signal levels high enough for the ADCs together with the drive amplifier having an adjustable gain. Recall, to minimize the effect of quantization noise and avoid the nonlinear distortion, the dynamic range of ADCs must be maximally exploited.

The output of Drive Amp, an RF bandpass signal, is fed into a quadrature mixer to extract the complex envelope that is an analog signal. After anti-aliasing lowpass filtering the I/Q components of complex envelope are digitalized by two 14-bit ADCs with a sampling rate of 100 MS/s. The sampling rate used by ADCs is converted into that of the Gigabit Ethernet network by downsampling and the digital I/Q samples of complex envelope are transferred to the host computer via Gigabit Ethernet for further signal processing.

**2. Transmit Block of USRP Device**

The transmit block starts with the host computer where I/Q components of the information bearing modulated waveforms are generated in baseband and then transferred over the Gigabit Ethernet to the FPGA of USRP device as shown in Fig. 8. The FPGA changes the sample rates according to the rates used by DACs and Gigabit Ethernet network. After upsampling, two 16-bit DACs operating at 400 MS/s convert the digital I/Q components of complex envelope into the analog domain. The analog I/Q components are low pass filtered to remove unwanted signal components and to limit the BB bandwidth in 40 MHz. The filtered analog I/Q components are fed into a quadrature mixer whose local signal is provided by a PLL. The quadrature mixer reconstructs the RF bandpass signal from its complex envelope and the RF output is amplified by a linear power amplifier having a variable gain. The RF output is available at the SMA connector Tx1.

**3. Implementation of Signal Processing Based on Complex Envelopes**

Figure 8 shows that the USRP device is a direct conversion transceiver [6]. A comparison of Figs. 3 and 4 with Fig. 8 reveals that in a mathematical sense the USRP device extracts the complex envelope of desired RF bandpass signal

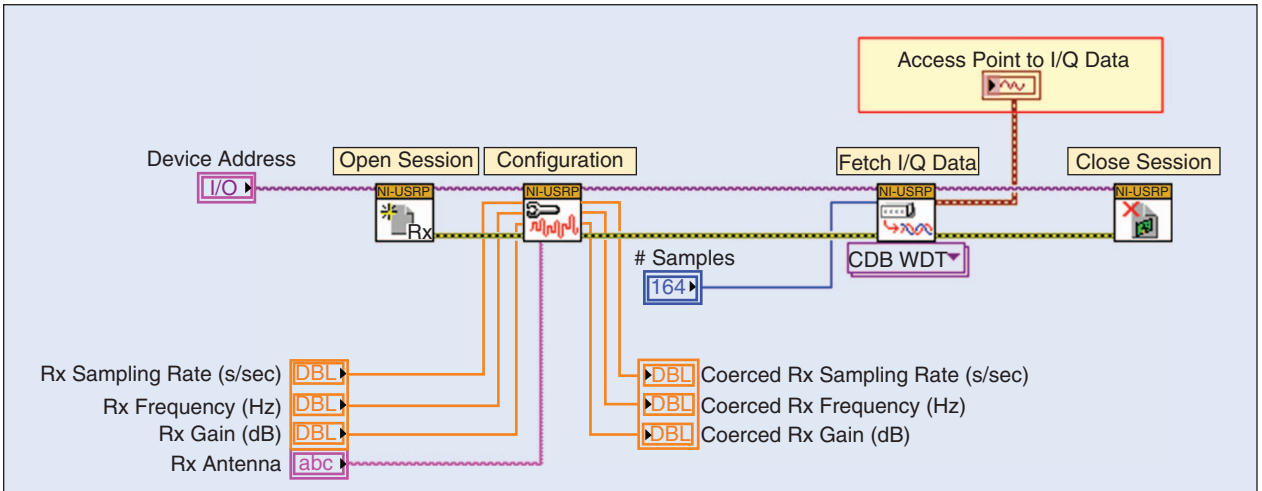


**Figure 9.** Complete control chain of the USRP device in receive mode.

at the receive side and reconstructs the RF bandpass signal from its complex envelope at the transmit side.

### *B. Software Platform for Accessing USRP Device*

One of the most efficient software platform to get access to the USRP device is LabVIEW [7], the SW platform used, that provides an extensive environment to implement *software defined electronics* starting with the control of USRP device, going on with the implementation of wireless communications systems and low-accuracy test equipment, finally, evaluating the system performance and measured data.

LabVIEW is a graphical programming environment that provides icons to perform any kinds of signal processing, data acquisition, even remote control of stand alone equipment. The USRP device implements the physical layer in the OSI basic reference (BR) model, consequently, it has to offer two kinds of services for the host-computer:

- USRP *management service* to set the USRP parameters such as receiver gain, carrier frequency, transmitted power, etc.;
- USRP *data service* to transfer the I/Q components of complex envelope.

The former can be done via the *configuration icons*, while the latter is performed by the *"Fetch I/Q Data"* and *"Write I/Q Data"* icons.

Software implementations of the complete control chain for accessing the USRP device are depicted in Figs. 9 and 10 for the receive and transmit mode, respectively. Each icon is identified by its function, written above the icon. Let the receive mode operation be considered first.

The USRP devices are identified by their IP addresses entered via the "Device Address" icon. This icon also opens the session with the USRP device. Then the following USRP parameters are entered via the "Configuration" icon:

- *Rx Sampling Rate [s/sec]:*
  Sample rate applied to the I/Q waveforms.
- *Rx Frequency [Hz]:*
  Assigns the RF carrier frequency.
- *Rx Gain [dB]:*
  Specifies the gain of RF amplifiers.
- *Rx Antenna:*
  Selects the transceiver configuration (duplex/simplex operation).

The constituting blocks of implemented USRP device do not allow the use of any arbitrary parameter combinations, certain restrictions apply. The USRP device keeps these parameters under control. If a desired parameter combination is not allowed then the USRP device selects the closest parameters available. These actual, referred to as *Coerced* parameters are returned by the "Configuration" icon.

The "Fetch I/Q Data" icon uploads the digitized complex envelope from the USRP device to the host-computer. It is also used to select the number of I/Q samples to be uploaded. Note, using the terminology of OSI model this icon provides the access point to the complex envelope of received RF bandpass signal. The "Access Point to I/Q Data" is marked by a red box in the figure. Finally, the "Close Session" icon terminates the session with the USRP device.

The control chain providing access to the USRP device in transmit mode is shown in Fig. 10. The two methods used in receive and transmit modes are nearly identical with a slight difference, in transmit mode the "Write I/Q Data" icon is used to download the digitized I/Q samples from the host-PC to the USRP device. Note, the notations Rx and Tx are used in Figs. 9 and 10 to distinguish the icons and parameters of receive and

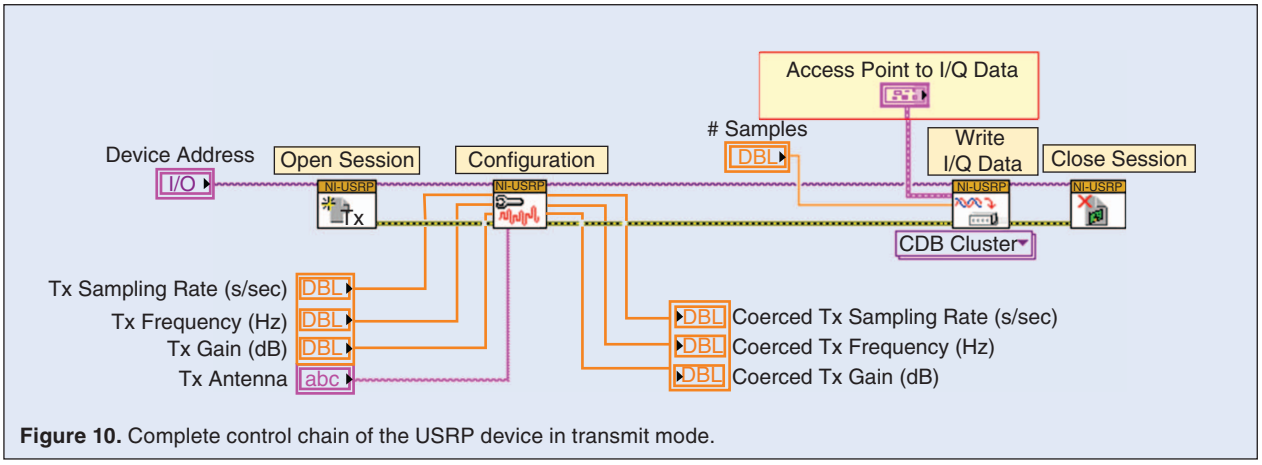


**Figure 10.** Complete control chain of the USRP device in transmit mode.

transmit modes, respectively. Again, the "Access Point to I/Q Data" is marked by a red box in Fig. 10.

### IV. Features of SW-Based BB Signal Processing

The theory of complex envelope approach has been discussed in Chapter II. Its main features are as follows:

- Every RF bandpass signal, either deterministic or random, can be fully *represented* in baseband by its complex envelope. Except the center frequency, the complex envelope carries all the information available in the original RF bandpass signal. Since the complex envelope represents its RF counterpart, it does *not involve* any distortion.
- Every RF bandpass signal, either deterministic or random, can be *reconstructed* from its complex envelope without any distortion.
- The complex envelope approach transforms the RF bandpass signal into baseband where it becomes a *lowpass signal*, consequently, it *assures the minimum sampling rate* which can be achieved. Theoretically, the sampling rate can be as low as the bandwidth of RF bandpass signal.
- An equivalent BB model can be derived for every RF bandpass system and algorithm.

The properties of complex envelope approach listed above make the implementation of any kind of RF transceiver or microwave test equipment possible in SW. There are two basic solutions to extract the complex envelope from an RF bandpass signal or to reconstruct it from its complex envelope: (i) the USRP approach discussed in Chapter III uses analog RF bandpass signals as input and output, while (ii) the FPGA-based Digital Down- and Upconverters (DDC and DUC, respectively) [8] rely on digitized input and output signals. The most important feature of these devices is that they are *universal HW devices* that can be used in any applications just by changing the SW used to perform the required signal processing.

The universal HW device and the SW are the constituting elements of *Software Defined Electronics*. Its main features are as follows:

- Very flexible, in a radio transceiver the modulation scheme and information processing (coherent/noncoherent, rake receiver, MIMO, etc.) can be changed dynamically;
- Easy solution to implement Software Defined Radio (SDR) and cognitive radio communications;
- Implementation of virtual instrumentation;
- Since the transmitted and received signals can be also used to test the radio transceiver and channel conditions, testing of radio transceiver and measurement of channel conditions can be performed parallel to radio communications, that is without interrupting the radio communications.

### V. Examples for the Derivation of BB Models, Implementation and Testing of a Complete Radio Link

This tutorial is devoted to the BB implementation of radio links including both the RF front-ends of the PHY layers and the radio channel. The upper layers can be also implemented in SW but the implementation of upper layers is out of scope of this material.

The constituting blocks of a radio link are as follows:

- *transmitter*, that converts the message to be transmitted, either analog or digital, into an analog waveform;
- *radio channel*, where the transmitted signal is corrupted by channel noise and may suffer from multipath and interference;
- *receiver*, that observes the corrupted received signal and recovers the message.

Similar to any HW-type conventional signal generator, the USRP is suitable for the generation of the required modulated waveform but the USRP approach can also implement the radio channel. The channel noise, interference

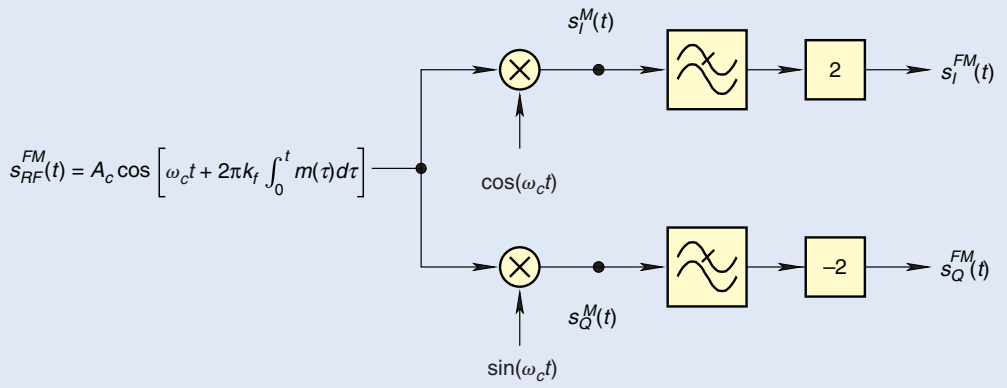


**Figure 11.** Derivation of BB equivalent of an analog FM modulator.

and effect of multipath propagation are implemented in BB and they are added to the complex envelope of modulated signal to be transmitted in SW. The USRP is driven by this composite complex envelope, consequently, the USRP output includes both the modulated signal and the channel effects. This capability, one of the main features of USRP approach, makes the use of an expensive channel sounder or RF noise generator unnecessary.

This chapter explains how a transceiver constituting the RF front-end of a PHY can be implemented in baseband. Two radio channels are considered, the AWGN channel and the noisy multipath channel. The interference, frequently modeled as a Gaussian process, can be implemented in the same way as the channel noise.

Both analog and digital modulators will be implemented. The radio propagation in AWGN and multipath radio channels will be modeled. After the implementation of a generic QPSK demodulator, the reception of noisy signals suffering from multipath will be demonstrated. The examples discussed in this chapter have been selected in such a way that each problem appearing in telecommunications is covered and after reading this chapter the reader will be able to derive the solution to his/her own problem.

As discussed in Chapter III two kinds of information have to be generated by the host computer in SW

- parameters of transceiver RF front-end to be implemented via the parameters of the USRP device such as receiver gain, transmitted power, carrier frequency, sampling rate, etc.;
- complex envelope that is transferred between USRP and host computer via Gigabit Ethernet network.

The parameters of USRP device are set via the user interface (Front Panel) provided by SW platform as it will be shown later in this Chapter. The complex envelopes are generated or processed by the host computer, this chapter shows the derivation of equivalent BB signal processing algorithms to be implemented in SW.

### *A. Analog FM Transmitter*

In frequency modulation, the instantaneous frequency deviation from a carrier $f_c$ is varied linearly with the message signal $m(t)$ [1]. The FM signal generated by the USRP device takes the form

$$s_{RF}^{FM}(t) = A_c \cos\left[2\pi f_c + 2\pi k_f \int_0^t m(\tau)d\tau\right], \qquad (19)$$

where $k_f$ denotes the frequency sensitivity of FM modulator, $A_c$ and $f_c$ are the amplitude and carrier frequency, respectively, of FM signal.

The steps of derivation of BB equivalent of an FM modulator are shown in Fig. 11 where the RF bandpass signal $s_{RF}^{FM}(t)$ is fed into the complex envelope generator depicted in Fig. 3. The output of the upper *in-phase arm* multiplier is obtained as

$$\begin{aligned} s_I^M(t) &= A_c \cos\left[\omega_c t + 2\pi k_f \int_0^t m(\tau)d\tau\right] \cos\omega_c t \\ &= \frac{A_c}{2}\left(\cos\left[2\pi k_f \int_0^t m(\tau)d\tau\right]\right. \\ &\quad \left. + \cos\left[2\omega_c t + 2\pi k_f \int_0^t m(\tau)d\tau\right]\right), \end{aligned} \qquad (20)$$

where the well-known "product-to-sum" trigonometric identity has been exploited. The ideal lowpass filter of Fig. 11 suppresses the sum frequency component on RHS and the in-phase component of complex envelope appears at the output of the amplifier having a gain of 2

$$s_I^{FM}(t) = A_c \cos\left[2\pi k_f \int_0^t m(\tau)d\tau\right]. \qquad (21)$$

The quadrature component is obtained in a similar manner

$$s_Q^{FM}(t) = A_c \sin\left[2\pi k_f \int_0^t m(\tau)d\tau\right]. \qquad (22)$$

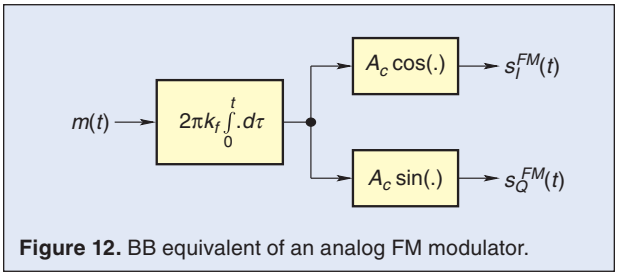


**Figure 12.** BB equivalent of an analog FM modulator.

The baseband equivalent of the analog FM modulator is depicted in Fig. 12.

Like any other signal processing task, the analog FM modulator can be implemented in two ways in the used SW platform:

- analog FM modulator of Modulation Toolkit can be used or
- BB equivalent shown in Fig. 12 can be constructed using elementary numeric and mathematical functions.

The used SW platform offers two graphical interfaces for the user [7], the *Block Diagram* and the *Front Panel*. The former is used to develop the source code while the latter one provides a custom design interface to enter the input data and visualize the computed and measured results. Since the development of source code is beyond the scope of this tutorial only the Front Panels of implemented systems will be shown.

Equivalent BB model depicted in Fig. 12 has been used to implement the analog FM modulator, the Front Panel of FM modulator is shown in Fig. 13. It is divided into two main panels, the parameters of FM modulator can be entered on the left panel while the complex envelope generated by SW is plotted on the right one.

The message signal $m(t)$ is a sinusoidal waveform, its frequency, the required frequency deviation and the number of generated samples can be entered on the left panel. The "STOP" button interrupts running the FM modulator program, while button of "Reconfigure" has to be pushed to enter the new parameters of FM modulation and/or USRP data.

The parameters of USRP device are entered into the left bottom subpanel of the left main panel. These parameters configure the transmit part of the USRP device via the configuration icons shown in Fig. 10. The following data are entered

- *Device Address:*
  IP address of selected USRP device;
- *Tx Sampling Rate [s/sec]:*
  Sampling rate of generated complex envelope in baseband;
- *Tx Frequency [Hz]:*
  Carrier frequency;
- *Tx Antenna:*
  Position of antenna switch;

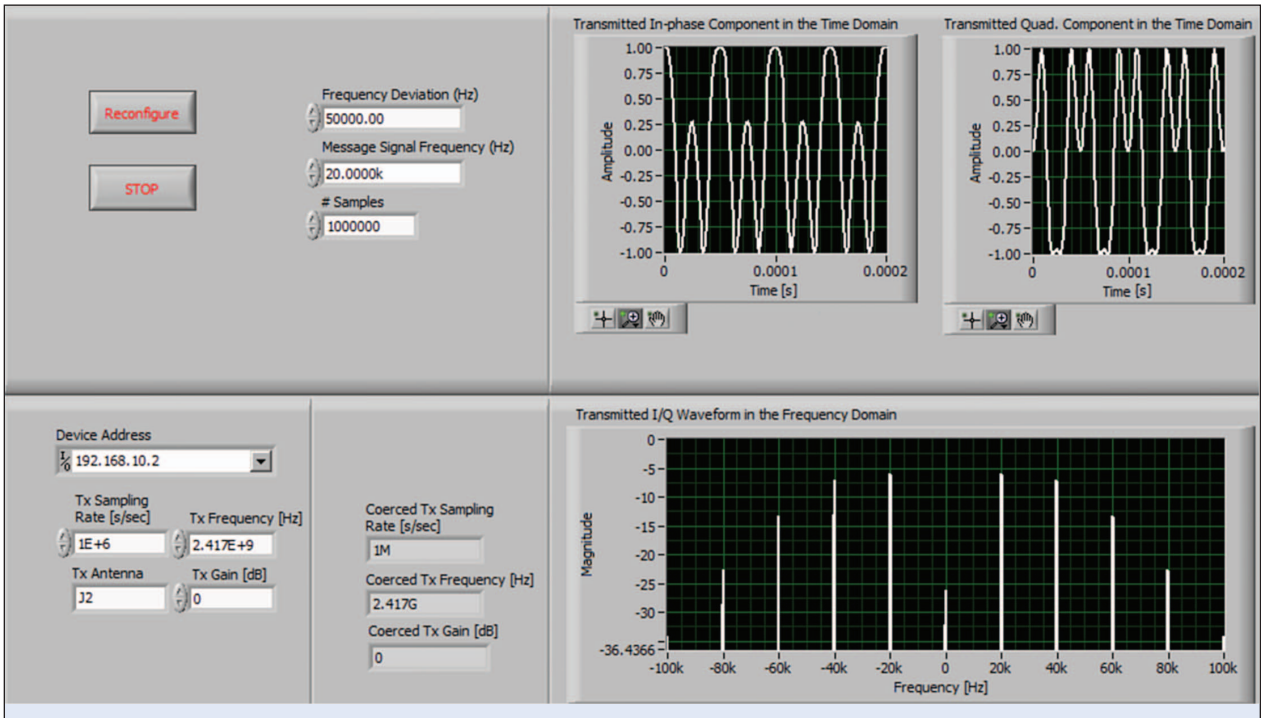


**Figure 13.** Front panel of FM modulator implemented in LabVIEW driving a USRP HW device.

- *Tx Gain [dB]:*
  Gain of transmitter. This parameter is used to set the transmitted power at the Tx1 output (refer to Fig. 8) of USRP device.

As explained in Chapter III, there are some internal limitations on the selectable parameter values used to configure the USRP device. The coerced parameter values are visualized on the right bottom subpanel.

The right main panel shows the generated complex envelope in the time- and frequency domains. The upper figures visualize the in-phase and quadrature components of generated complex envelope while the power spectrum of generated complex envelope is shown in the lower figure.

To check the usability of USRP approach and the validity of equivalent BB model depicted in Fig. 12, a stand alone spectrum analyzer was connected to the RF output of USRP device in order to check the spectrum of generated FM signal in the RF domain. The measured spectrum is shown in Fig. 14. The setting of spectrum analyzer can be recovered from the figure. Note, the shape of BB spectrum shown on the Front Panel of Fig. 13 and that of measured by the stand-alone spectrum analyzer are identical verifying the statement that any RF signal processing task can be substituted by an equivalent one in baseband.

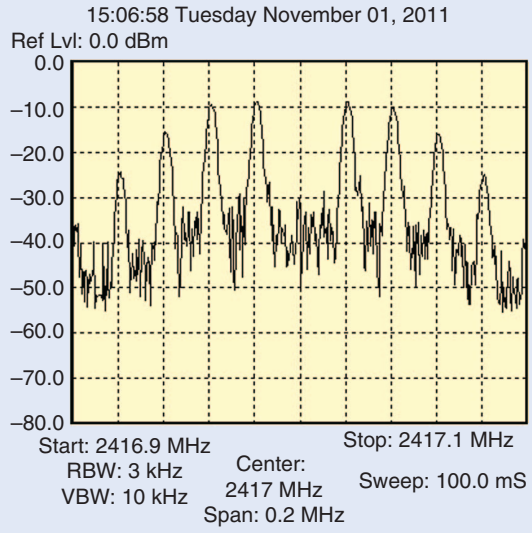


**Figure 14.** RF spectrum of the implemented USRP FM modulator measured by a stand alone spectrum analyzer.

### *B. AWGN Radio Channel*

The block diagram of a bandpass AWGN radio channel [1] is depicted in Fig. 15 where $s(t)$ and $y(t)$ are the transmitted signal before and after, respectively, the channel attenuation. The received signal $r(t)$ is corrupted by the channel noise $w(t)$, a white Gaussian random process characterized by its psd $N_0/2$.

In AWGN channel the channel attenuation $K$ is determined by the Friis formula [9], where the channel attenuation is expressed as a function of receiver's distance from the transmit antenna, carrier frequency and the gains of transmit and receive antennas.

The complex envelope approach can be applied only to bandpass signals and systems. Consequently, the white Gaussian noise denoted by $w(t)$ has to be band limited by a bandpass filter as depicted in Fig. 15, where $2B_{\text{noise}}$ is the RF bandwidth of filtered noise $n(t)$.

The band limiting filtering does not restrict the validity of our investigation because in practice we have to consider only bandpass signals. If the bandwidth $2B_{\text{noise}}$ of filtered channel noise $n(t)$ is much larger than that of the signals of interest, including both the desired signal and interferences, then the bandpass filtering does not restrict the validity of our model.

In digital implementation or in computer simulation, the bandpass filtering is not explicitly implemented many times. In that case the RF bandwidth is determined by the sampling frequency $2B_{\text{noise}} = f_s$.

The derivation of BB equivalent of RF bandpass AWGN channel model requires the establishment of a direct relationship between the complex envelope of transmitted signal $s(t)$ and that of the received signal $r(t)$. The former and latter are denoted by $s_I(t)$–$s_Q(t)$ and $r_I(t)$–$r_Q(t)$, respectively. The derivation of BB equivalent will be presented here as a step-by-step process.

In Step One, the RF bandpass model is completed by the block diagrams provided in Chapter II to reconstruct an RF bandpass signal from its complex envelope and to extract the complex envelope from an incoming RF bandpass signal. The former and latter block diagrams are shown in Figs. 4 and 3, respectively. The result of Step One is depicted in Fig. 16.

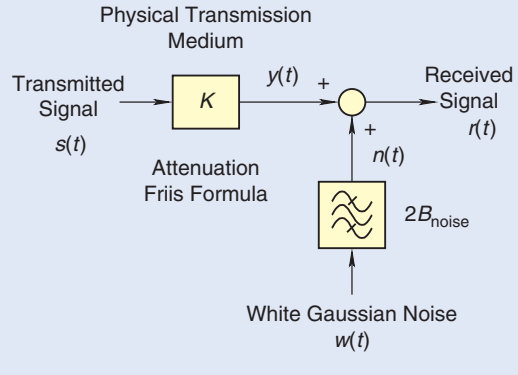


**Figure 15.** Block diagram of a bandpass AWGN radio channel in the RF domain.

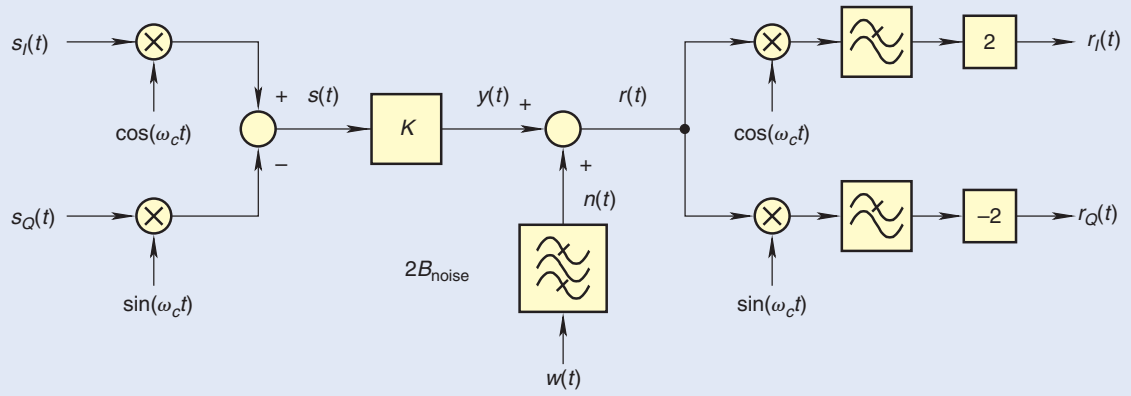


**Figure 16.** Derivation of BB equivalent, Step One.

In Step Two the rules of block diagram algebra are used to move the generation of channel noise and RF channel attenuation into the baseband. The result of Step Two is depicted in Fig. 17.

Inspecting Fig. 17 we can recognize that $n_I(t)$ and $n_Q(t)$ denoted by dots in Fig. 17 are the in-phase and quadrature components of complex envelope of band-limited channel noise $n(t)$. Note, the Gaussian noise $n(t)$ is not a white noise, it has been derived from the Gaussian white channel noise $w(t)$ by an RF bandpass filter as shown in Fig. 15. As discussed in Sec. II-F, the $n_I(t)$- and $n_Q(t)$-components of complex envelope of $n(t)$ can be

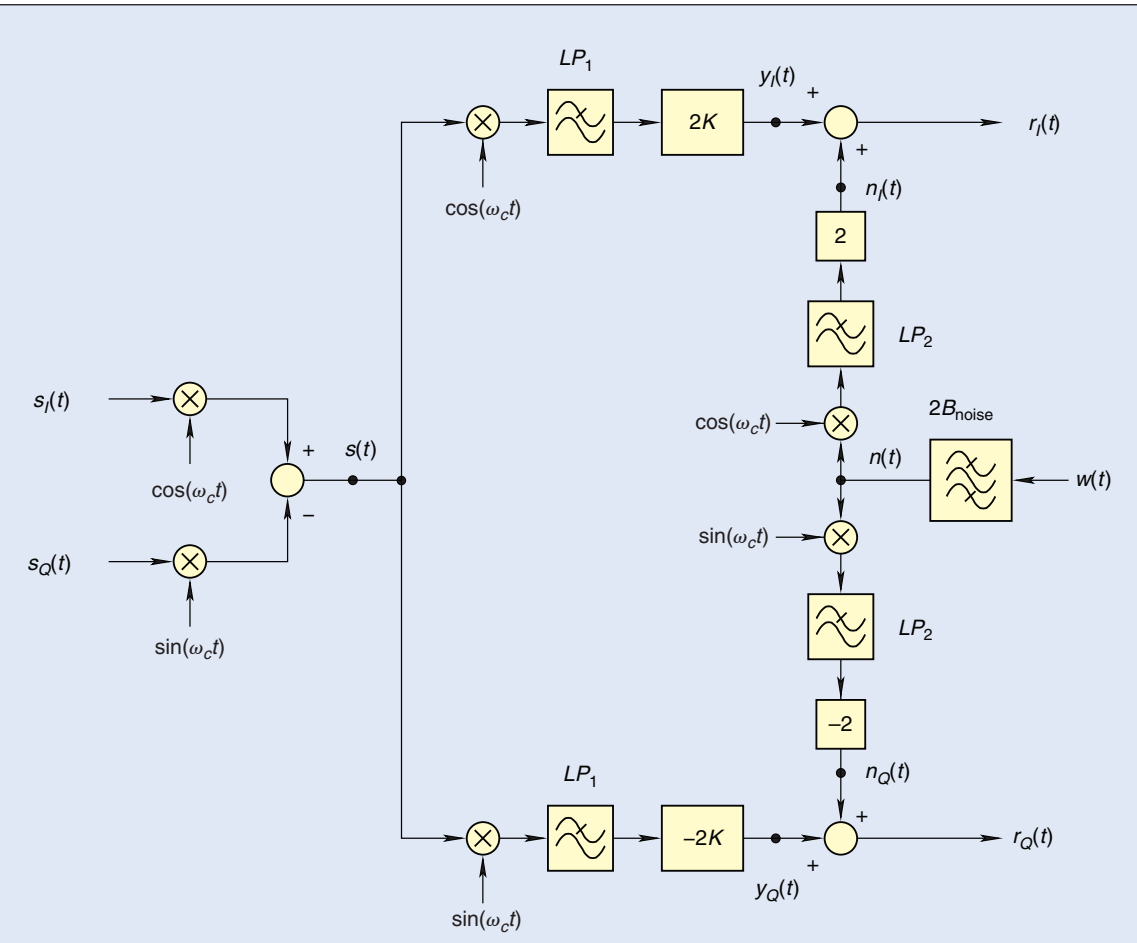


**Figure 17.** Derivation of BB equivalent, Step Two.

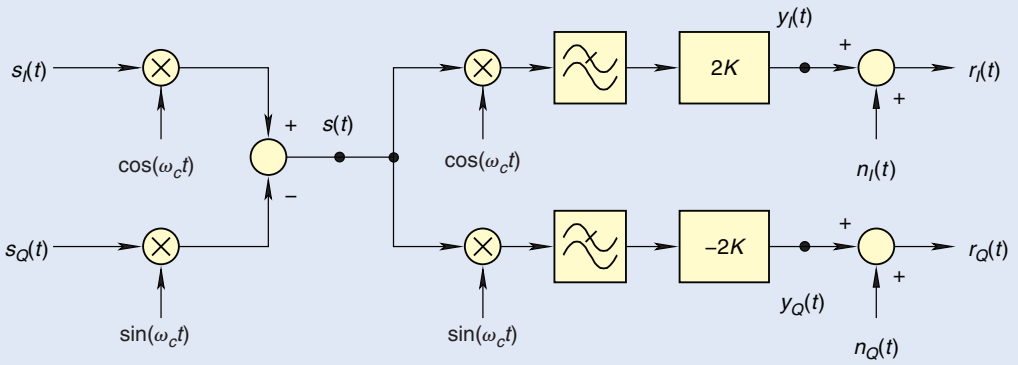


**Figure 18.** Derivation of BB equivalent, Step Three.

generated directly in baseband, consequently, Fig. 17 can be further simplified to Fig. 18.

Finally, the direct relationships between $r_I(t)$–$r_Q(t)$ and $s_I(t)$–$s_Q(t)$ have to be established. Note, the block diagram depicted in Fig. 18 is linear related to the complex envelopes, consequently, the superposition theorem may be applied. Applying the product-to-sum trigonometric identity first, then exploiting the frequency shifting property of Fourier transform (also referred to as modulation theorem), the response generated in $y_I(t)$ by the in-phase component $s_I(t)$ is obtained as

$$y_I^{[s_I]}(t) = \mathcal{LP}[s_I(t)\cos^2(\omega_c t)]\times 2K = 2K\times \mathcal{LP}\left[s_I(t)\frac{1+\cos(2\omega_c t)}{2}\right] = K s_I(t), \quad (23)$$

where function $\mathcal{LP}[\cdot]$ expresses the filtering effect of the two lowpass filters used in Fig. 18 to suppress the sum-frequency output of the multipliers and $\times$ denotes multiplication.

The effect of $s_Q(t)$ on $y_I(t)$ is zero because

$$y_I^{[s_Q]}(t) = \underbrace{\mathcal{LP}[-s_Q(t)\sin(\omega_c t)\cos(\omega_c t)]}_{=0}\times 2K = 0. \quad (24)$$

In a similar way $y_Q(t)$ can be expressed as functions of $s_I(t)$ and $s_Q(t)$

$$y_Q(t) = K s_Q(t). \quad (25)$$

Exploiting the results of (23), (24) and (25), Figure 18 can be further simplified. The equivalent BB model of RF AWGN channel is shown in Fig. 19 where the random processes $n_I(t)$ and $n_Q(t)$ are generated directly in baseband. Their statistical parameters are determined by applying the equations given in Sec. II-F. Recall, $n_I(t)$ and $n_Q(t)$ must be orthogonal random processes. Any correlation measured between the two random signals seriously destroys the spectral properties of generated channel noise and the validity of measurements or computer simulation.

Using the block diagram depicted in Fig. 19, an AWGN channel simulator has been implemented in LabVIEW and the RF bandpass signal has been reconstructed by the USRP device. The Front Panel of the implemented AWGN channel simulator is shown in Fig. 20. Note, the sampling rate and bandwidth of generated bandpass Gaussian noise can be set independently of each other. First two Gaussian PRN sequences are generated, the orthogonality of them is assured by entering different seeds into the PRNGs. Then both PRN sequences are processed by two independent low-pass filters in order to set the RF bandwidth of channel noise to $2B_{\text{noise}}$. The two lowpass filters are also implemented in SW, their frequency responses can be clearly identified in Fig. 20.

The number of noise samples to be processed in one cluster and the standard deviation of generated noise

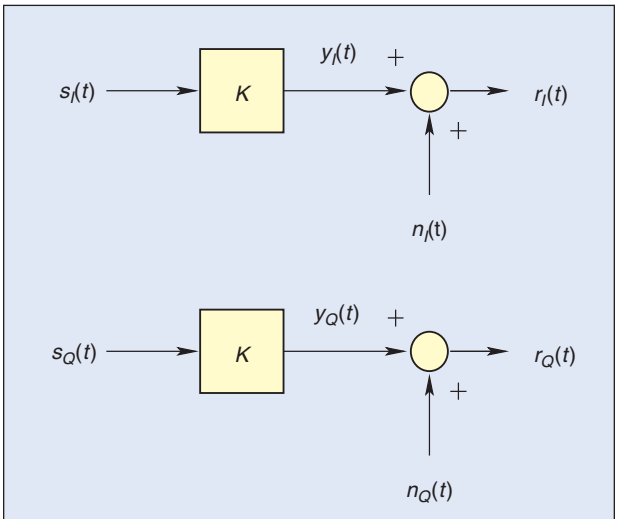


**Figure 19.** BB equivalent of AWGN channel. Recall, $n_I(t)$- and $n_Q(t)$-components must be orthogonal random processes.

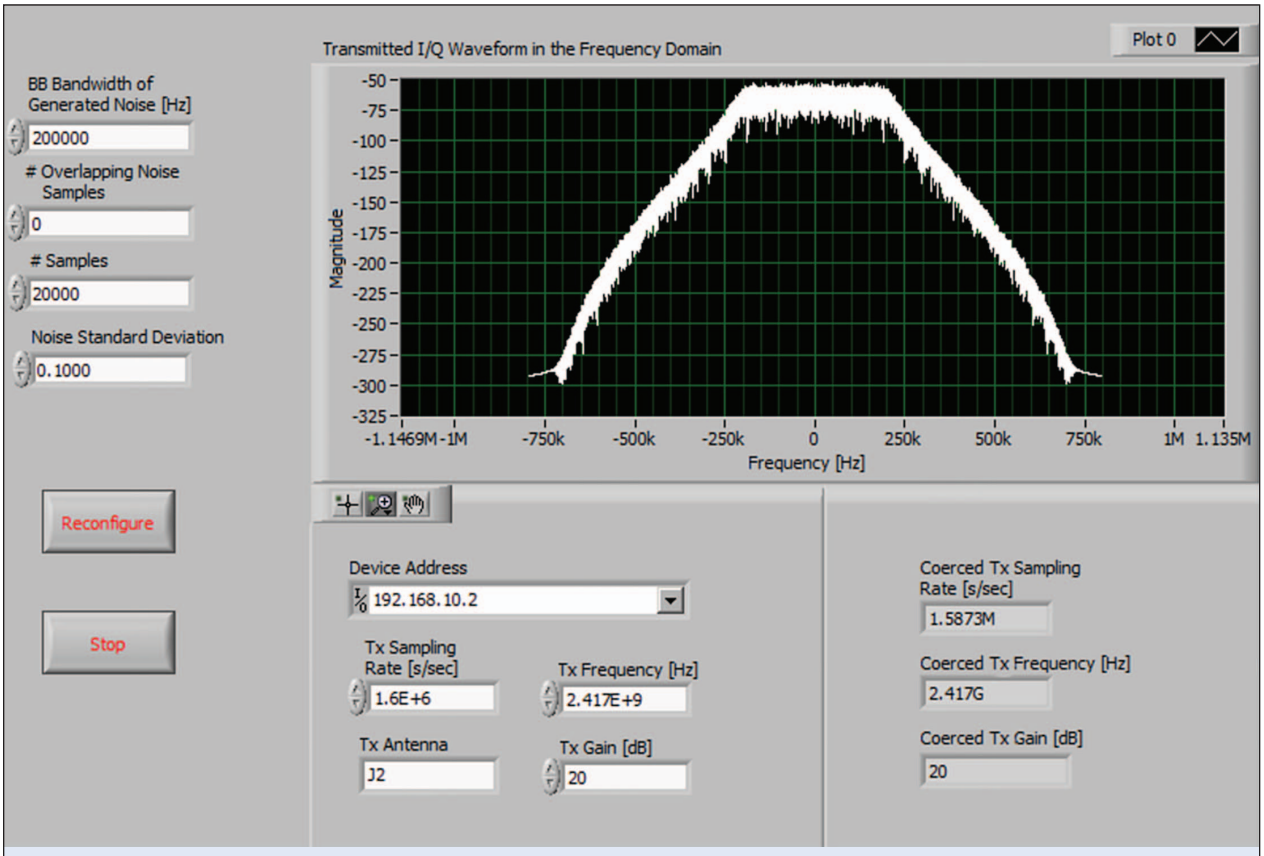


**Figure 20.** Front panel of AWGN channel simulator implemented in LabVIEW using USRP HW device.

can be set from the Front Panel. The standard deviation and RF bandwidth of generated channel noise together determine the noise power. As expected and shown in Fig. 20 the psd of generated noise is constant in the baseband. Consequently, the BB model derived here is really suitable to implement an AWGN channel in the frequency band covered by the spectra of the signals of interest.

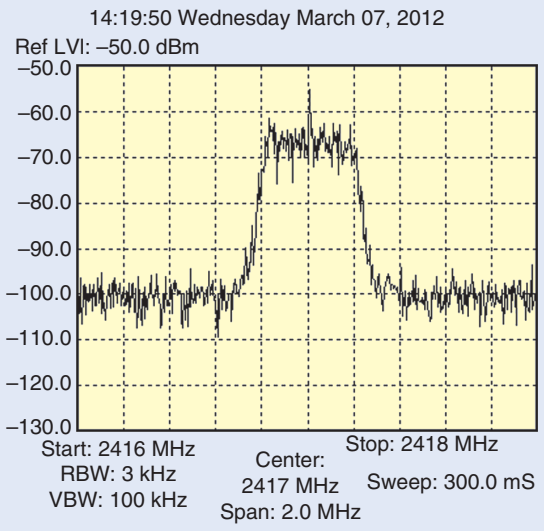


**Figure 21.** RF spectrum of generated channel noise measured by a stand alone spectrum analyzer.

To verify the theory, the channel noise generated at the USRP output has been measured by a stand alone spectrum analyzer. Figure 21 proves that, as expected, a bandpass noise with constant psd has been generated in the RF domain. The center frequency and RF bandwidth of noise are 2.417 GHz and 400 kHz, respectively. A spike can be observed at 2.417 GHz, that is caused by the local leakage in the USRP quadrature mixer.

Until this time the USRP device operated in the linear region. If an RF circuit is driven into the nonlinear region then the phenomenon of spectral regrowth can be observed [6]. If our theory is correct then the phenomenon of spectral regrowth should also appear in the USRP approach.

The easiest way to overdrive the USRP device is to increase the standard deviation of noise in baseband. The RF power spectrum of noise with increased standard deviation is shown in Fig. 22. Except the standard deviation all the parameters of AWGN channel simulator were kept constant. A comparison of Figs. 21 and 22 shows clearly the effect of nonlinear distortion, as expected,

new spectral components on both sides of the original spectrum are emerging.

### *C. Two-Ray Multipath Channel*

Multipath propagation is modeled by *tapped delay line model* [10] where each propagation path is characterized by its delay and gain. For the sake of simplicity a two-ray noisy multipath channel is considered here where the gain and delay of the main path are set to zero.

BB model of two-ray multipath channel can be derived across the steps discussed in Sec. V-B. First the RF tapped delay line model is completed with the block diagrams establishing the relationship between the RF bandpass signals and their complex envelopes. This block diagram is depicted in Fig. 23, where the gain and delay of the second propagation path are $k_2$ and $T_2$, respectively.

Next the direct relationships between $r_I(t)$–$r_Q(t)$ and $s_I(t)$–$s_Q(t)$ have to be found. Since the block diagram depicted in Fig. 23 is linear, the superposition theorem can be applied.

The signal path between $s_I(t)$ and $r_I(t)$ can be followed in Fig. 23. Applying the product-to-sum trigonometric identity first, then exploiting the frequency shifting property of Fourier transform, the response generated in $r_I(t)$ by the in-phase component $s_I(t)$ is obtained as

$$\begin{aligned} r_I^{[s_I]}(t) &= 2\times\mathcal{LP}[(s_I(t)\cos(\omega_c t) \\ &\quad + k_2 s_I(t-T_2)\cos[\omega_c(t-T_2)])\cos(\omega_c t)] \\ &= s_I(t) + k_2 s_I(t-T_2)\cos(\omega_c T_2), \end{aligned} \tag{26}$$

where function $\mathcal{LP}[\,\cdot\,]$, as before, describes the effect of lowpass filtering.

The effect of $s_Q(t)$ on $r_I(t)$ is obtained in a similar manner

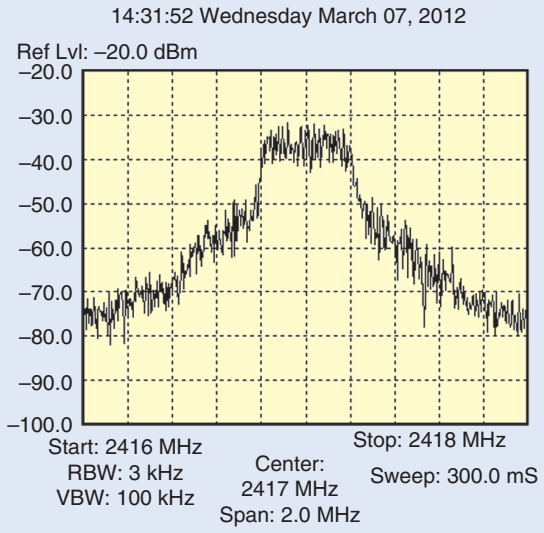


**Figure 22.** Spectral regrowth observed in the RF region when USRP is driven into saturation.

$$\begin{aligned} r_I^{[s_Q]}(t) &= 2\times\mathcal{LP}[(-s_Q(t)\sin(\omega_c t) \\ &\quad - k_2 s_Q(t-T_2)\sin[\omega_c(t-T_2)])\cos(\omega_c t)] \\ &= k_2 s_Q(t-T_2)\sin(\omega_c T_2). \end{aligned} \tag{27}$$

Finally $r_Q(t)$ is expressed as functions of $s_I(t)$ and $s_Q(t)$

$$r_Q(t) = s_Q(t) + k_2 s_Q(t-T_2)\cos(\omega_c T_2) - k_2 s_I(t-T_2)\sin(\omega_c T_2). \tag{28}$$

To get a compact notation (26)–(28) are rewritten as

$$\begin{bmatrix} r_I(t) \\ r_Q(t) \end{bmatrix} = \begin{bmatrix} s_I(t) \\ s_Q(t) \end{bmatrix} + k_2 \underbrace{\begin{bmatrix} \cos(\omega_c T_2) & \sin(\omega_c T_2) \\ -\sin(\omega_c T_2) & \cos(\omega_c T_2) \end{bmatrix}}_{=\mathbf{D}} \begin{bmatrix} s_I(t-T_2) \\ s_Q(t-T_2) \end{bmatrix}, \tag{29}$$

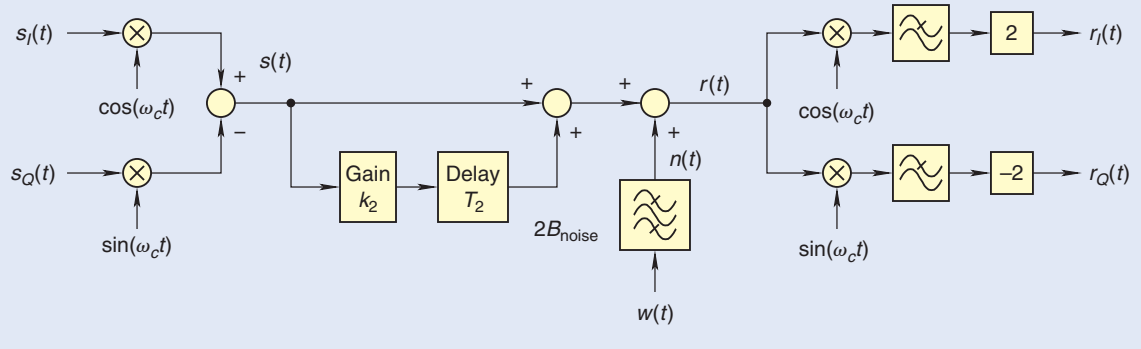


**Figure 23.** Derivation of BB equivalent of a two-ray noisy multipath channel. Completing the RF model with the two blocks establishing the relationship between the RF signals and their complex envelopes.

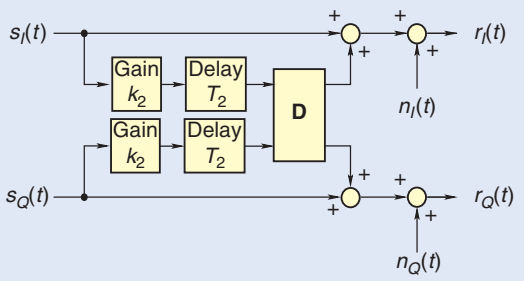


**Figure 24.** BB equivalent of a two-ray noisy multipath channel. Note the cross-coupling between the in-phase and quadrature arms.

where the elements of delay matrix **D** are constant but their values depends on the product of the delay of path two and center frequency.

Equation (29) reveals why multipath propagation is so harmful in digital communications:

- Multipath propagation causes a cross-coupling between the in-phase and quadrature arms. This cross coupling is described by the delay matrix **D**.
- Digital modulations such as QPSK, QAM relay on in-phase and quadrature components and, consequently, are very sensitive to multipath because it causes a cross coupling between the information bearing signal components.
- For $\omega_c T_2 = 2k\pi, k = 0, 1, \ldots$ $\mathbf{D} = \mathbf{I}$ and the cross-coupling between the two propagation paths becomes zero.

The BB equivalent of two-ray noisy multipath channel is constructed by combining (29) with the derivation of BB model of AWGN channel depicted in Fig. 19. The BB model developed is shown in Fig. 24. Note again, the channel noise always has to be added directly to the received signal $r(t)$.

### *D. Generic BB Model of QPSK/O-QPSK Modulators*

Due to the page limit, only the QuadriPhase-Shift Keying [1] (QPSK, also referred to as Quadrature Phase-Shift Keying) and Offset QPSK [11] modulation schemes are considered here. However, the approach presented here can be applied to $M$-ary PSK and QAM modulations.

The generic block diagram of QPSK and O-QPSK modulation schemes is depicted in Fig. 25 where $b_i, i = 1, 2, \cdots$ is the data stream to be transmitted, $p(t)$ denotes the impulse response of pulse shaping filter (also referred to as transmit filter in the literature) and $s_i(t)$ is the modulated RF bandpass signal. Note, different kinds of data encoders can be used in the implemented systems, in the solution shown in the figure the incoming bit stream is decomposed into two bit streams, the upper and lower bit streams carry the even and odd bits, respectively.

In O-QPSK a half-sine pulse shaping filter is used and the lower bit stream is delayed by $T_S/2$, half of symbol duration. In QPSK modulators the time delay $T_S/2$ has to be set to zero.

The equivalent BB model of generic QPSK/O-QPSK RF modulator is obtained by inspection. Comparison of Figs. 4 and 25 shows that

$$I_{BB}(t) = x_I(t)$$

and

$$Q_{BB}(t) = -x_Q(t).$$

Considering these equations, the BB equivalent of generic QPSK/O-QPSK modulator can be constructed as shown in Fig. 26.

Based on the BB equivalent model derived above, a generic QPSK/O-QPSK RF modulator has been developed. The Front Panel of the software developed is shown in Fig. 27 where a QPSK modulator with raised cosine pulse shaping is implemented.

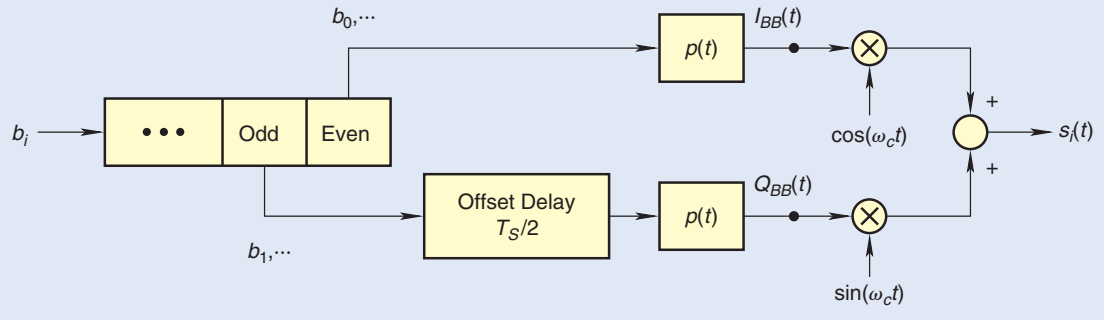


**Figure 25.** Generic block diagram of a QPSK/O-QPSK RF modulator. The time delay $T_S/2$ has to be set to zero in case of QPSK modulators.

The Front Panel is partitioned into two main panels, the left and right panels are used to enter the parameters of generic modulator and to visualize the signals in baseband, respectively. The left main panel is divided into three subpanels that, from the top to the bottom, are used to select the parameters of USRP, modulation scheme and channel conditions. The selection of USRP parameters have been explained in Sec. V-A and is not repeated here, setting of channel conditions will be shown later in this section.

The following parameters can be entered via the middle subpanel:

- *Number of Bits:*
  Number of bits to be transmitted;
- *PSK Type:*
  Select the desired modulation scheme. Choices available: QPSK and O-QPSK;
- *Pulse Shaping Filter:*
  Select the desired pulse shaping filter. Choices available: ZoH, raised cosine and half sine;
- *Symbol Rate [sym/sec]:*
  Number of symbols transmitted per second;
- *Raised Cos Filt Param:*
  Rolloff factor of raised cosine filter;
- *Samples/Symbol:*
  Number of I/Q samples in one symbol;
- *I/Q Gain:*
  Sets the amplitude of I/Q waveform.

On the right main panel the generated BB waveforms are visualized. The two waveforms on the left top shows the in-phase and quadrature components of generated complex envelope. Next to them the constellation diagram is visualized where the message points, i.e., the values of transmitted signal at the decision time instants are shown in red. The subpanel on the bottom gives the power spectrum of generated QPSK signal in baseband.

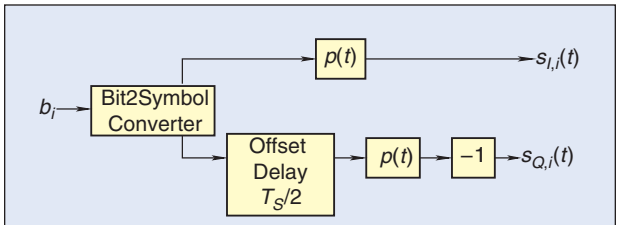


**Figure 26.** BB equivalent of generic QPSK/O-QPSK modulator. The time delay $T_S/2$ has to be set to zero in case of QPSK modulators.

The complex envelope generated in SW has been fed into the USRP device to reconstruct the modulated RF bandpass signal. The spectrum of reconstructed RF signal has been checked by a stand alone spectrum analyzer, the measured spectrum is shown in Fig. 28. The settings of spectrum analyzer can be recovered from the figure. Note, an ideal channel has been selected on the Front Panel (see Fig. 27, left bottom subpanel), consequently, the waveforms and spectra shown in Figs. 27 and 28 belong to the noise-free case.

An extremely important feature of USRP approach is that not only the modulated waveform but even the *propagation conditions* can implemented in baseband. As an example, consider the problem where the output of an O-QPSK modulator, implemented with a half-sine pulse shaping filter, propagates via an AWGN channel. The RF output of USRP device should include both O-QPSK modulation and the effect of AWGN channel.

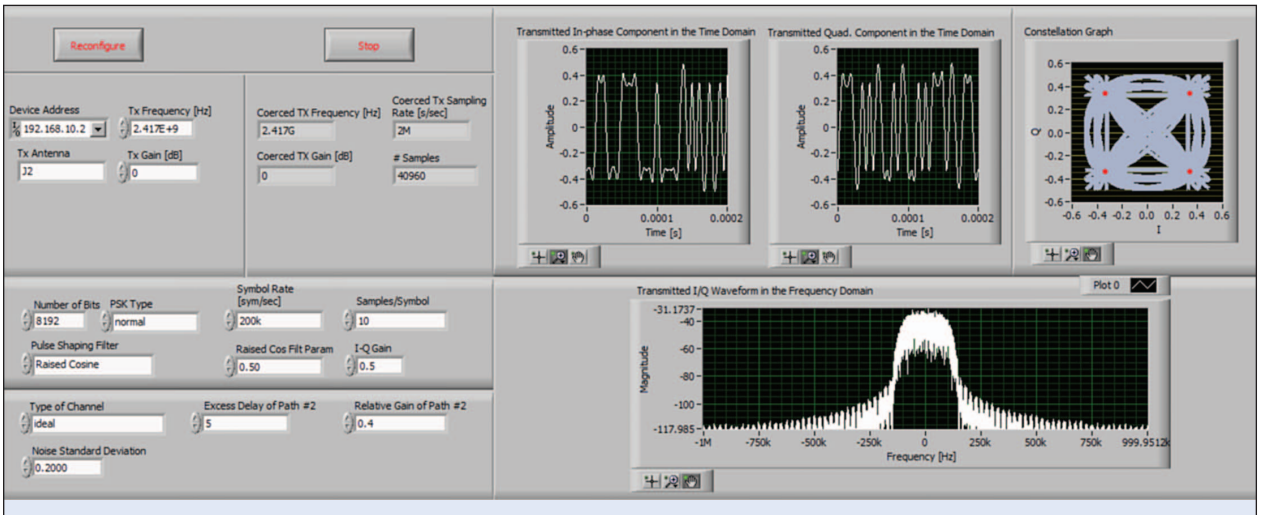


**Figure 27.** Front panel of a QPSK modulator built with raised cosine pulse shaping.

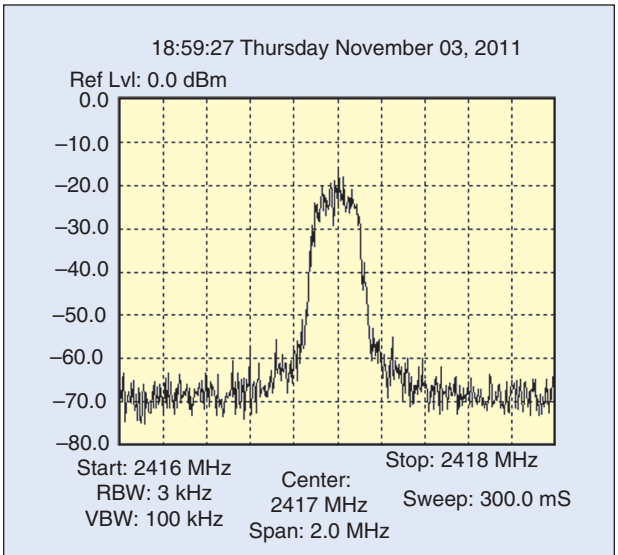


**Figure 28.** RF spectrum of generated QPSK signal measured by a stand alone spectrum analyzer. Raised cosine pulse shaping with a roll-off factor of 0.5 has been used to form the spectrum of QPSK signal.

To get the BB equivalent of this system configuration, the block diagrams derived to model the generic QPSK/O-QPSK modulator and effect of noisy multipath channel, see Figs. 26 and 19, respectively, are connected in cascade. The Front Panel, shown in Fig. 29, is identical to that of the generic QPSK/O-QPSK BB modulator. The fields provided to enter the data of USRP unit and parameters of modulation have been already explained above, here only the duty of the bottom subpanel on the left is discussed.

The left bottom subpanel provides the access to the type and parameters of radio channel. The following fields are available:

- *Type of Channel:*
  Select the type of channel. Choices available: Ideal, AWGN, noise-free multipath, noisy multipath channels;
- *Noise Standard Deviation:*
  Determines the psd of channel noise, i.e., the noise floor;
- *Excess Delay of Path #2:*
  Delay of path #2 in samples;
- *Relative Gain of Path #2:*
  The gain of path #2.

The presence of channel noise can be clearly recognized on the constellation diagram of Fig. 29 where a Gaussian cloud appears about each message point. The effect of channel noise can be also observed in the figure shown on the right bottom subpanel where the power spectrum of noisy O-QPSK signal is visualized in baseband. Note, the channel noise has a uniform psd in the bandwidth of interest and the noise floor hides a large part of the spectrum of O-QPSK signal.

The RF spectrum of noisy O-QPSK signal generated by the USRP device has been checked by a stand alone spectrum analyzer. The measured spectrum is shown in Fig. 30, the settings of spectrum analyzer are given in the figure. Note, the RF channel noise has a uniform psd over the bandwidth observed and the SNR is so bad that, as expected, the noise floor hides a very large part of the spectrum of O-QPSK signal.

Consider a half-sine O-QPSK transmitter communicating via a noisy two-ray radio channel. The BB model of this configuration is obtained by connecting in cascade the BB equivalents of generic QPSK/O-QPSK modulator shown in Fig. 26 and noisy multipath channel depicted in Fig. 24. The Front Panel and the generated complex

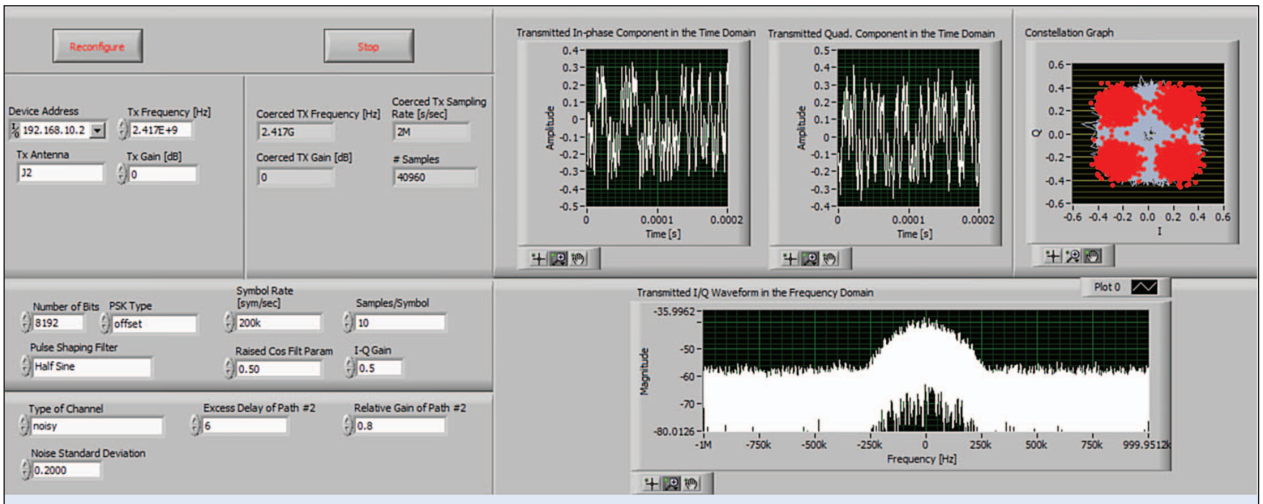


**Figure 29.** Implementation of an O-QPSK modulator together with an AWGN channel. A half-sine pulse shaping filter is used to form the spectrum of transmitted signal.

envelope both in the time- and frequency-domains are visualized in Fig. 31 where a noisy multipath channel with $k_2 = 0.5$ and $T_2 = 2.5\ \mu$s have been selected. Note, delay of path two is obtained as a product of "*Excess Delay of Path #2*" and "*Coerced IQ Rate*."

The parameters of path two have been selected in such a way that

$$\frac{\omega_c T_2}{2\pi} = k = 6042.5,$$

consequently, $\mathbf{D} = -\mathbf{I}$ and the cross-coupling between the two propagation paths becomes zero.

The presence of additive channel noise can be clearly observed in both the constellation diagram and the BB spectrum. The multipath propagation causes frequency selective fading, its appearance can be seen in the BB spectrum around the zero frequency.

The spectrum of generated RF signal available at the USRP output is shown in Fig. 32, where the settings of stand alone spectrum analyzer can be recovered from the figure. As expected both the channel noise and the multipath-related frequency selective fading appear around the carrier frequency.

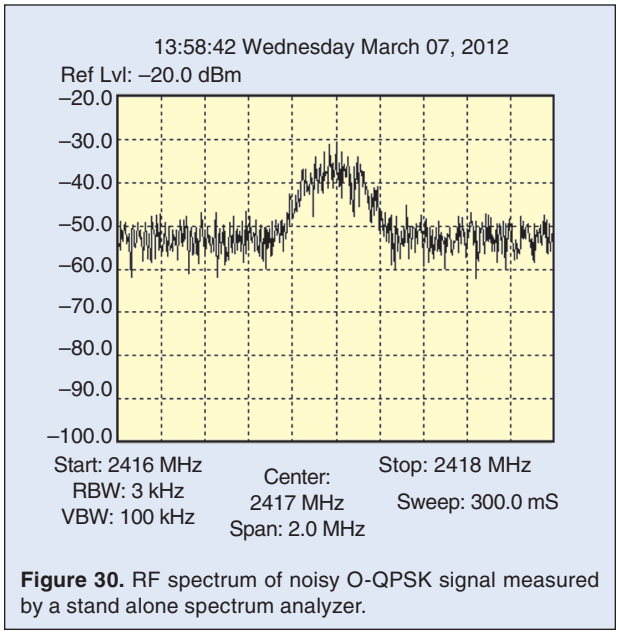


**Figure 30.** RF spectrum of noisy O-QPSK signal measured by a stand alone spectrum analyzer.

### *E. Implementation and Testing of a Complete Radio Link*

Each radio link includes

- a transmitter
- a radio channel
- a receiver.

This section will implement a generic QPSK/O-QPSK receiver and establish a complete radio link communicating over a noisy two-ray multipath channel. To implement a stand-alone transmitter and a stand-alone receiver, two USRP devices and two PCs are used in an isolated manner, where Configuration #1, one USRP device and one PC, implements the transmitter and the noisy two-ray multipath channel, while Configuration #2 implements the receiver and measures both the spectrum and constellation diagram of received signal.

The block diagram of test bed including both the transmitter and receiver is shown in Fig. 33. The random bit sequence to be transmitted is generated at the transmitter and sent via a USB interface to the receiver for evaluation purposes, for example, to determine the Bit Error Rate (BER). The RF modulated waveform generated by the transmitter is fed via a coaxial cable into the

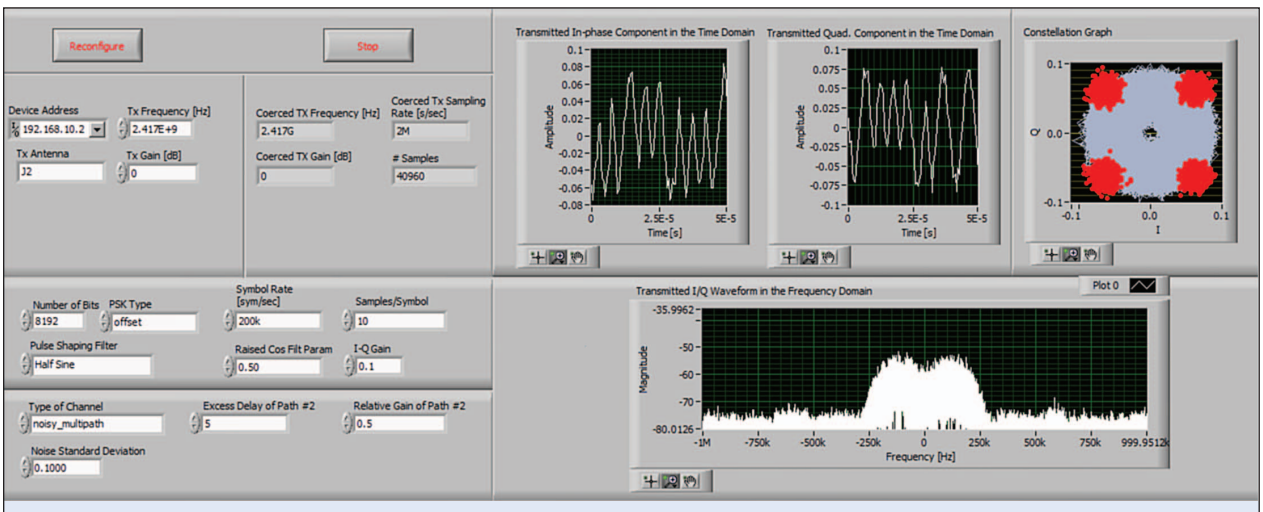


**Figure 31.** Implementation of an O-QPSK modulator together with a noisy two-ray multipath channel. A half-sine transmit filter is used for pulse shaping.

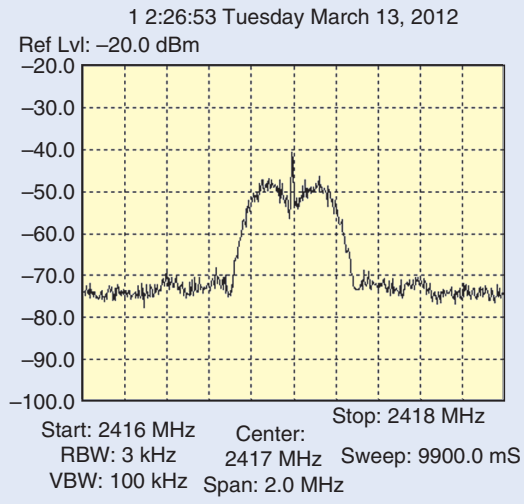


**Figure 32.** RF spectrum of an O-QPSK signal transmitted via a noisy two-ray multipath channel. The power spectrum has been measured by a stand alone spectrum analyzer.

receiver. A 20-dB attenuator is used between the transmitter and receiver to provide sufficient isolation.

A half-sine O-QPSK modulator together with a noisy two-ray multipath channel have been implemented in Sec. V-D, the Front Panel of the simulator is shown in Fig. 31. That configuration will be used by Configuration #1 to implement the transmitter and simulate the radio channel.

Generic block diagram of QPSK and O-QPSK receivers [1], [12] is depicted in Fig. 34, where $r(t)$ denotes the RF bandpass received signal corrupted by channel noise and multipath effects. The carrier recovery circuits recovers the orthonormal basis functions from the received modulated signal [13]. The output of two correlators constituting the coherent QPSK receiver are denoted by $R_I(t)$ and $R_Q(t)$. These signals are fed into decision circuits, the decision time instants are assigned by the output of a symbol-timing recovery, also referred to as clock recovery circuit [13]. The estimated bit stream $\hat{b}_i$ is recovered by the data decoder.

In Figure 34, $T_S$ denotes the symbol time period. The decision for a symbol is performed at the same time instant in both the in-phase and quadrature channels in QPSK, however, in offset QPSK the sampling is delayed by the half of symbol period in the in-phase channel. This delay is also shown in the figure, for QPSK the delay has to be set to zero.

The equivalent BB model of generic QPSK/O-QPSK RF receiver can be obtained by inspection. Comparison of Figs. 3 and 34 shows that

$$R_I(t) = \frac{x_I(t)}{2}$$

and

$$R_Q(t) = -\frac{x_Q(t)}{2}.$$

Applying these equations, the BB equivalent of generic QPSK/O-QPSK receiver can be obtained as shown in Fig. 35 where $r_I(t)$ and $r_Q(t)$ denotes the in-phase and quadrature components, respectively, of complex envelope of received signal $r(t)$.

A radio link includes both a transmitter and a receiver. Based on the BB equivalent model derived above, a generic QPSK/O-QPSK RF receiver has been developed and implemented by Configuration #2. The received RF band pass signal $r(t)$ has been generated by Configuration #1, and the two stand alone configurations have been connected by a coaxial RF cable. The bit stream to

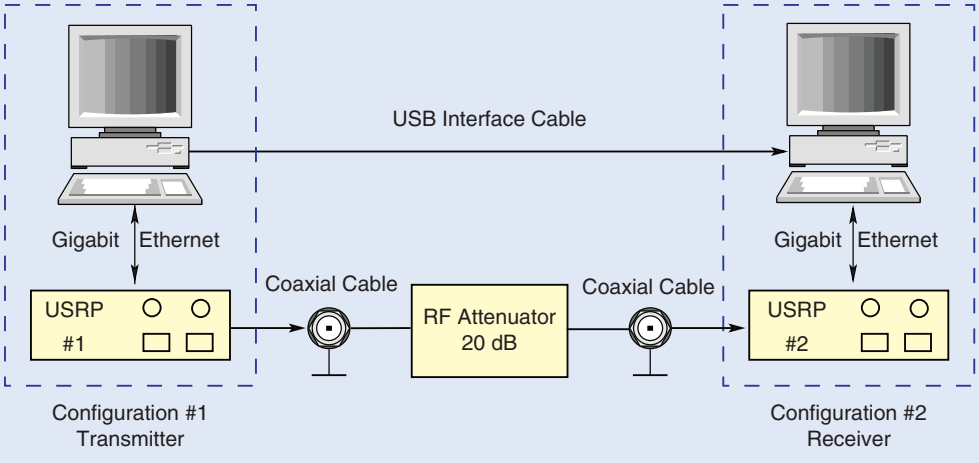


**Figure 33.** Block diagram of test bed developed to test a complete radio link.

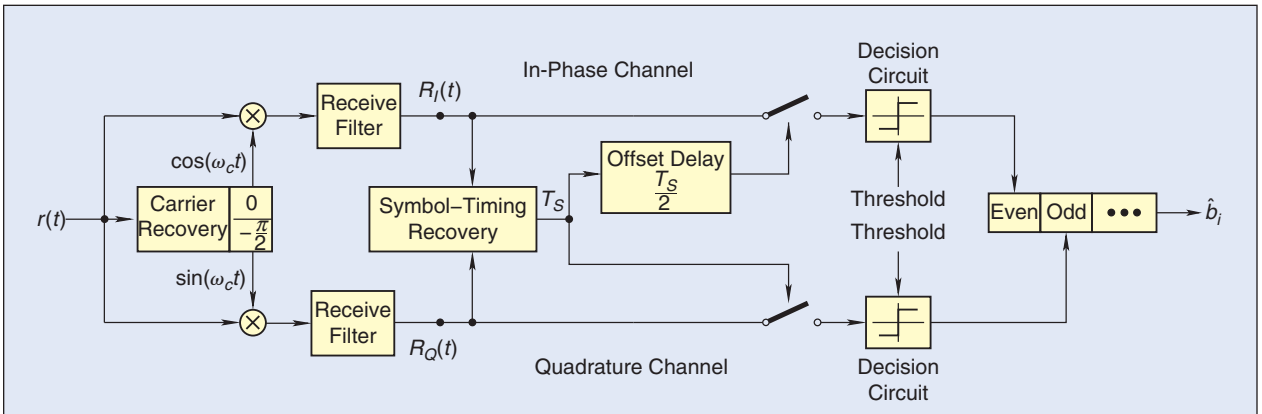


**Figure 34.** Generic block diagram of QPSK/O-QPSK receiver. The offset delay $T_S/2$ has to be set to zero in QPSK.

be transmitted has been generated by Configuration #1, implementing the transmitter, and has been provided to Configuration #2, used as a receiver, via a USB interface. Recall, the Front Panel of the half sine O-QPSK transmitter is depicted in Fig. 31.

The Front Panel of the software developed to implement the receiver is shown in Fig. 36. This receiver is the counterpart of the implemented O-QPSK transmitter of Fig. 31, the meaning of fields already explained are not repeated here.

As shown in Fig. 36, the Front Panel of generic QPSK/O-QPSK receiver is divided into three main panels: the (i) top, (ii) middle and (iii) bottom panels.

On the left side of top panel the parameters of USRP device are entered. The carrier recovery is performed by an algorithm that needs to know the parameters of QPSK modulator used to generate the signal to be demodulated. These parameters, namely the type of modulator, the type and parameters of pulse shaping filter and the number of samples taken in one symbol period are entered in the middle part of the top panel. On the right side of top panel the transmitted and recovered bit streams are visualized. The transmitted bit stream is *a priori* known and passed from the PC used to implement the transmitter to the other one that implements the receiver via a USB interface. The recovered bit stream is estimated by the generic QPSK/O-QPSK demodulator implemented in SW. The comparison of two bit sequences gives the BER performance.

The middle panel plots the signals measured in the demodulator. The left oscillograms depict the in-phase and quadrature components of complex envelope of received signal in white and red colors, respectively. The figure on the right side visualize the eye diagram. The effects of channel noise and multipath propagation can be well observed, they reduce the openness of eye diagram considerably.

One of the most important features of software defined electronics is that any kinds of signal processing can be implemented by this approach including radio

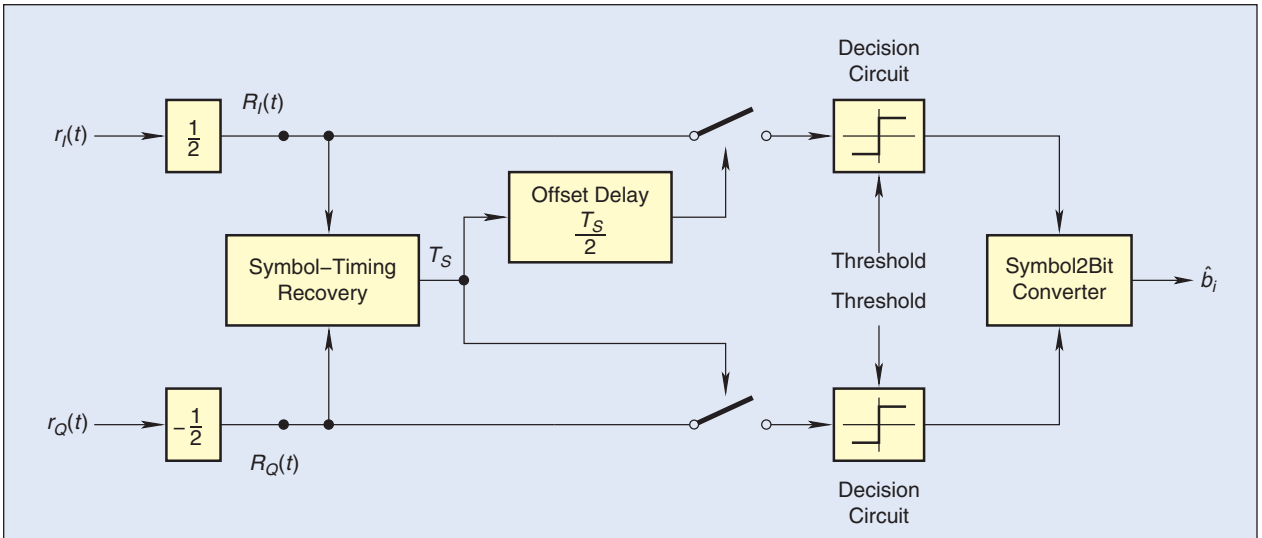


**Figure 35.** BB equivalent of generic QPSK/O-QPSK receiver. The offset delay $T_S/2$ has to be set to zero in QPSK.

transceivers or test equipment. Because the transmitted signal carries not only the useful information but it also can be considered as a test signal, both the receiver and the test equipment can be implemented by software and the reception of desired signal and testing the radio link can be performed simultaneously, without interrupting the data traffic.

To demonstrate this feature, two test equipment have been implemented in software. The measured results are visualized on the bottom panel of Front Panel as shown in Fig. 36.

The figure on the left depicts the spectrum of received signal. Note, the effect of noisy multipath channel can be clearly observed

- a deep multipath-related fading is present about the zero frequency in baseband (recall, zero frequency corresponds to the carrier frequency in the RF domain)
- sidebands of received modulated signal are partially lost in the channel noise.

The spectrum of noisy half-sine O-QPSK signal suffering from multipath is determined by three different manner and shown by three different equipment:

- on the Front Panel of transmitter software that is visualized on the computer screen belonging Configuration #1, see Fig. 31
- on the stand alone spectrum analyzer screen depicted in Fig. 32
- on the Front Panel of Configuration #2 that implements the half-sine O-QPSK receiver, see Fig. 36.

As expected, the three spectra are identical. This verifies the statement that any kinds of RF bandpass signal, either deterministic or random, and any kinds of LTI systems can be implemented in baseband exploiting the theory of complex envelopes and using the USRP approach.

The constellation diagram measured at the half-sine O-QPSK receiver is visualized on the right side of bottom panel. As expected, due to the channel noise and

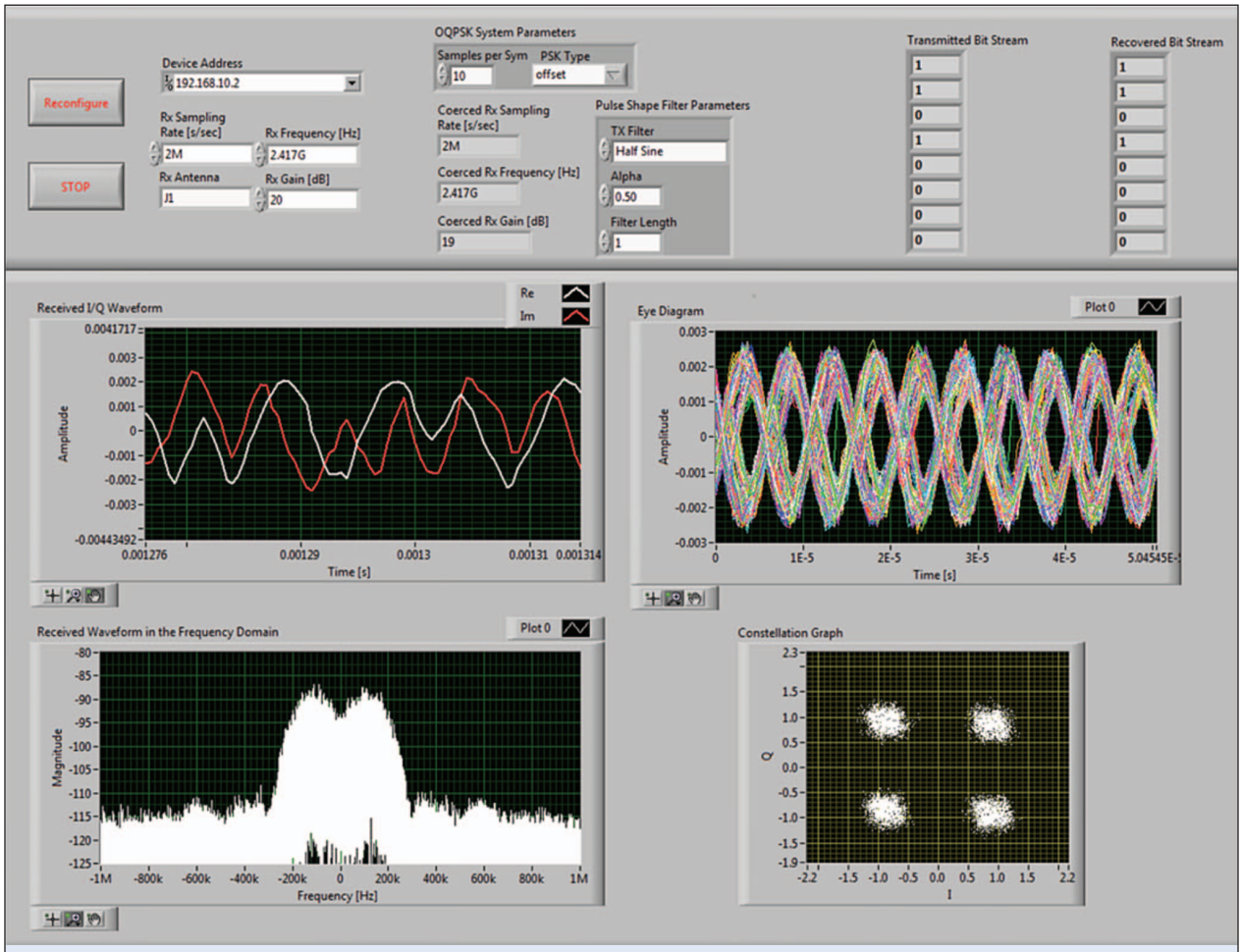


**Figure 36.** Implementation of an O-QPSK receiver. The received signal is distorted by a noisy two-ray multipath channel.

**Software Defined Electronics (SDE) offers a flexible implementation environment where both the functionality and all parameters of an application can be changed by software.**

multipath propagation, a Gaussian cloud forms about each message point.

Recall, the eye diagram, spectrum of received signal and constellation diagram are used during the performance test of digital telecommunications systems to measure, check and evaluate their performance. The channel properties also can be determined from these measurements, consequently the channel information that is crucial in software defined and cognitive radio also can be recovered. Even more, this information is continuously available and can be extracted without the interrupting the data traffic.

## VI. Conclusions

Software defined and cognitive radios, virtual instrumentation require a flexible implementation environment where both the *functionality* of application and the *parameters* of application can be changed by software. Examples for the former and latter are the modulation scheme and the data rate, respectively. This goal can be achieved by the SDE approach where a universal HW device and a host computer are used to implement the desired application. According to the OSI BR model the universal HW device and host computer implement the PHY and application layers, respectively.

In telecommunications and measurement engineering the high sampling rate and resolution required are the main challenges. In the SDE approach every RF bandpass signal processing is substituted by its BB equivalent using the concept of complex envelopes. The bandwidth of BB equivalent is equal to the half of the RF bandwidth, consequently, the sampling rate is determined by the RF bandwidth and not by the RF center frequency.

In the USRP approach, a universal HW device is used (i) to extract the complex envelope of the RF bandpass signal to be processed and (ii) to reconstruct the RF bandpass signal from its complex envelope. The processing of complex envelope is performed by the host computer. Always the same universal HW device is used, the implementation of a new application requires only to change the SW on the host computer. Today the universal HW devices and the programming environment are available, the only challenge is the derivation of the equivalent BB signal processing algorithms.

This tutorial surveyed the theory of complex envelopes and introduced the USRP approach as the universal hardware platform of implementing arbitrary RF bandpass telecommunications systems and measurement equipment. A step-by-step approach was introduced for the derivation of equivalent BB model of analog and digital transceivers, channel noise and multipath noisy propagation environment. The power of SDE concept was demonstrated by many examples starting from a simple case, the implementation of an analog FM modulator, and finishing with the most complex set up where an entire half-sine O-QPSK transceiver communicating over a noisy multipath channel was implemented.

A unique feature of SDE concept is that many parallel signal processing tasks running simultaneously can be implemented on the same host computer. This feature was also demonstrated in the half-sine O-QPSK radio link implemented where in addition to the demodulation the received signal was considered as an excitation and was used to test the radio link and measure the channel conditions.

In many applications not a host computer but an FPGA device will be used to implement the application SW. The CAS Society is expected to develop equivalent BB algorithms for the different applications that can be used in an optimum manner in the FPGA environment.

## VII. Acknowledgments

The USRP devices and LabVIEW software used to implement the examples presented in the tutorial have been donated by the National Instruments. This work has been sponsored by the Hungarian Scientific Research Found (OTKA) under Grant number T-084045 and supported by the Automated Testing Ltd., Budapest, Hungary. The author would like to convey their thanks to the support, without that this work would not have been successful.

**Géza Kolumbán** (M'92, SM'98, FIEEE'05) is currently a professor in the Faculty of Information Engineering of Pázmány Péter Catholic University, Budapest, Hungary.

He received his M.Sc. (1976) and Ph.D. (1990) degrees from the Technical Univ. of Budapest, C.Sc. (1990) and D.Sc. (2004) degrees from the Hungarian Academy of

Sciences, and Dr.habil degree (2005) from the Budapest Univ. of Technology and Economics. After his graduation, he spent 15 years in professional telecommunications industry, where he developed microwave circuits and PLL-based frequency synthesizers. He was involved in many system engineering projects such as SCPC-type satellite telecommunication system, microwave satellite up- and down-converters, low-capacity microwave digital radio system, etc. After joining the university education, he elaborated the theory of chaotic waveform communications and established noncoherent chaotic communications as a brand new research direction. He developed DCSK and FM-DCSK, the most popular chaotic modulation schemes. Two of his papers, coauthored with Profs. M.P. Kennedy and L.O. Chua, have been ranked in top-cited IEEE Trans. CAS-I articles. His publications have been cited more than 1900 times. He has been a visiting professor and researcher to UC Berkeley, PolyU and CityU in Hong Kong, University College Dublin and Cork, Ireland, EPFL, Switzerland, INSA-LATTIS Laboratory, Toulouse, France, TU Dresden, Germany. He has been providing consulting service for many companies, for National Instruments, Austin, USA and Samsung, Suwon, Korea, etc. Prof. Kolumban is the cofounder of Automated Testing for RF and Microwaves Ltd that, based on virtual instrumentation, develops automated test systems for the industry.

**Tamás István Krébesz** (Member, IEEE) received the M.Sc. degree from the Budapest University of Technology and Economics in 2007. He is currently working toward the Ph.D. degree at the Department of Measurement and Information Systems.

He has been an academic visitor and research assistant to The Hong Kong Polytechnic University (PolyU) and INSA-LATTIS Laboratory, Toulouse, France. His current research and professional interests include computer simulation of ultra-wideband radio, chaos communications, networking devices of embedded systems and automated measurement system providing traceability. He is the cofounder of Automated Testing for RF and Microwaves Ltd.

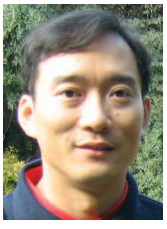

**Francis C.M. Lau** received the B.Eng. (Hons) degree in electrical and electronic engineering and the PhD degree from King's College London, University of London, UK. He is a Professor and Associate Head at the Department of Electronic and Information Engineering, The Hong Kong Polytechnic University, Hong Kong. He is also a senior member of IEEE.

He is the coauthor of *Chaos-Based Digital Communication Systems* (Heidelberg: Springer-Verlag, 2003) and *Digital Communications with Chaos: Multiple Access Techniques and Performance Evaluation* (Oxford: Elsevier, 2007). He is also a co-holder of three US patents, one pending US patent, and one international patent. He has published over 200 papers. His main research interests include channel coding, cooperative networks, wireless sensor networks, chaos-based digital communications, applications of complex-network theories, and wireless communications.

He served as an associate editor for *IEEE Transactions on Circuits and Systems II* in 2004–2005 and *IEEE Transactions on Circuits and Systems I* in 2006–2007. He was also an associate editor of *Dynamics of Continuous, Discrete and Impulsive Systems, Series B* from 2004 to 2007, a co-guest editor of *Circuits, Systems and Signal Processing* for the special issue "Applications of Chaos in Communications" in 2005, and an associate editor for *IEICE Transactions (Special Section on Recent Progress in Nonlinear Theory and Its Applications)* in 2011. He has been a guest associate editor of *International Journal and Bifurcation and Chaos* since 2010 and an associate editor of *IEEE Circuits and Systems Magazine* since 2012.

## References


[1] S. Haykin, *Communication Systems,* 3rd ed. New York: Wiley, 1994.

[2] J. D. Gibson, Ed. *The Mobile Communications Handbook,* 2nd ed. Boca Raton, FL: CRC, 1999.

[3] M. P. Fitz, *Fundamentals of Communications Systems*. New York: McGraw-Hill, 2007.

[4] J. O. Smith, *Introduction to Digital Filters with Audio Applications*. W3K Publishing, 2007.

[5] NI Universal Software Radio Peripheral (USRP). National instruments [Online]. Available: http://sine.ni.com/nips/cds/view/p/lang/en/nid/209947

[6] B. Razavi, *RF Microelectronics.* Upper Saddle River, NJ: PTR Prentice Hall, 1998.

[7] LabVIEW System Design Software. National instruments [Online]. Available: http://www.ni.com/labview/

[8] Xilinx Digital Up- and Down-Converter (DUC and DDC) Solutions, DUC/DDC Compiler. Xilinx [Online]. Available: http://www.xilinx.com/products/intellectualproperty/DUC DDC Compiler.htm

[9] H. T. Friis, "A note on a simple transmission formula," *Proc. IRE*, vol. 34, p. 254, 1946.

[10] J. G. Proakis, *Digital Communications*. Singapore: McGraw-Hill, 1995.

[11] J. A. Gutiérrez, E. H. Gallaway, and R. L. Barett, *Low-Rate Wireless Personal Area Networks: Enabling Wireless Sensors with IEEE 802.15.4,* 3rd ed. Standards Information Network, IEEE Press, 2011.

[12] B. McGuffin and P. Kwong, "I/q channel reversal correcting properties of an SQPSK Costas loop with integrated symbol synchronization," *IEEE Trans. Commun*., vol. 36, pp. 1082–1086, Sept. 1988.

[13] G. Kolumbán, "Phase-locked loops," in *The Encyclopedia of RF and Microwave Engineering*, vol. 4, K. Chang, Ed. Hoboken, NJ: Wiley, 2005, pp. 3735–3767.